

# Design of an Infrared based Blood Oxygen Saturation and Heart Rate Monitoring Device

by

Yousuf Jawahar

Electrical and Biomedical Engineering Project Report (4BI6)  
Department of Electrical and Computer Engineering  
McMaster University  
Hamilton, Ontario, Canada

# Design of an Infrared based Blood Oxygen Saturation and Heart Rate Monitoring Device

by

Yousuf Jawahar

Department of Electrical and Computer Engineering  
Faculty Advisor: Prof. Doyle

Electrical and Biomedical Engineering Project Report  
Submitted in partial fulfillment of the requirements  
for the degree of Bachelor of Engineering

McMaster University  
Hamilton, Ontario, Canada  
April 10, 2009  
Copyright © March 2009 by Yousuf Jawahar

## **ABSTRACT**

The purpose of the project was to design a remote non-invasive health monitoring system. Health information would be collected and transferred to a processing centre wirelessly, where it can be monitored and forwarded to necessary personnel. Heart Rate and Blood Oxygen Saturation are a couple of such biometrics that are monitored in this project. Change in intensity of light transmitted through tissue due to arterial blood pulse can be measured as a voltage signal. This technique is called Photoplethysmography (PPG), and can be used to calculate the heart rate. Furthermore, oxygenated blood has different light absorption characteristics than deoxygenated blood under Red and Infrared wavelengths. Comparing the two absorptions can produce an estimate of the oxygen saturation of the blood. Time Multiplexing was used to collect the two PPGs (Red and Infrared) simultaneously. The hardware design and the software processing required to measure these biometrics will be presented.

Keywords: photoplethysmography, PPG, oxygen saturation, pulse oximetry, heart rate, time multiplexing

## **ACKNOWLEDGEMENTS**

The author would like to thank his team members Mastan Kalsi, Omer Waseem, and Aiyush Bansal for their support and creative ideas through out the project, Dr. Doyle<sup>1</sup> for his guidance, and Dr. Noseworthy<sup>2</sup> for his words of encouragement and for providing the team with a commercial pulse oximeter during the testing phase.

---

<sup>1</sup> Dr. Thomas E. Doyle, P. Eng, Assistant Professor, ECE Dept., McMaster University

<sup>2</sup> Dr. Michael D. Noseworthy, Ph.D., Scientist and MRI Physicist, Imaging Research Centre, St. Joseph's Healthcare

## TABLE OF CONTENTS

Abstract.....	ii
Acknowledgements.....	iii
Table of Contents.....	iv
List of Tables.....	v
List of Figures.....	vi
List of Figures.....	vi
Nomenclature.....	vii
<b>1 Introduction.....</b>	<b>1</b>
1.1 Objectives.....	1
1.2 Scope and Methodology.....	2
<b>2 Literature Review.....</b>	<b>3</b>
2.1 Transmittance vs. Reflectance.....	3
2.2 Wavelengths of light.....	5
<b>3 Problem Statement and Methodology of Solution.....</b>	<b>6</b>
3.1 Theory of PPG and Heart Rate.....	6
3.2 Theory of Blood Oxygen Saturation.....	7
3.3 Problem Statement.....	9
3.4 Methodology of Solution.....	10
<b>4 Design Procedures.....</b>	<b>12</b>
4.1 LED circuits and Photodiode selection.....	12
4.2 Current to Voltage Converter.....	13
4.3 Preamplifier.....	15
4.4 Signal Filtering.....	16
4.5 Time Multiplexing.....	20
4.6 555/556 Timer.....	25
4.7 Decade Counter.....	27
4.8 Sample and Hold Circuits.....	31
4.9 Timing Circuit.....	32
4.10 Summing Amplifier.....	33
4.11 Serial Port to TCP/IP interface.....	34
4.12 Heart Rate Calculation.....	38
4.13 Blood Oxygen Saturation Calculation.....	38
<b>5 Results and Discussion.....</b>	<b>41</b>
5.1 Testing Procedures.....	41
5.2 Circuitry Testing Results.....	43
5.3 Heart Rate Data Processing Results.....	47
5.4 Blood Oxygen Saturation Data Processing Results.....	49
<b>6 Conclusions and Recommendations.....</b>	<b>52</b>
<b>7 Appendix A: Hardware Cost and Prototype.....</b>	<b>54</b>
<b>8 Appendix B: Data Processing Software.....</b>	<b>56</b>
8.1 MATLAB Processing Code.....	56
8.2 Ruby TCP/IP Server code.....	57
<b>9 References.....</b>	<b>60</b>
<b>10 Vitae.....</b>	<b>61</b>

## LIST OF TABLES

Table 1: Extinction coefficient ( $\epsilon$ ) of haemoglobin .....	8
Table 2: Bill of Materials .....	54

## LIST OF FIGURES

Figure 1: Transmittance and Reflectance configurations of transducer .....	3
Figure 2: Light Absorption characteristics of HbO <sub>2</sub> and Hb at different wavelengths.....	5
Figure 3: PPG waveform demonstrating blood dynamic features .....	7
Figure 4: LED/Photodiode signal testing.....	12
Figure 5: Current to voltage converter.....	14
Figure 6: Inverting Preamplifier .....	15
Figure 7: Passive Band pass filter with Amplification .....	17
Figure 8: Active Band-pass filter.....	19
Figure 9: Magnitude Transfer function of Active BPF.....	19
Figure 10: Phase transfer function of Active BPF .....	19
Figure 11: Multithreading.....	21
Figure 12: Time sharing affects of Multithreading.....	21
Figure 13: Sampling of signals in Time Multiplexing.....	23
Figure 14: 555/556 Timer circuit generating 1.1KHz clock signal .....	26
Figure 15: State machine of Time Multiplexing.....	27
Figure 16: Improved state machine for Time Multiplexing.....	28
Figure 17: Signal output from Decade Counter.....	29
Figure 18: Decade Counter state machine for Time Multiplexing .....	30
Figure 19: Decade Counter Circuit.....	30
Figure 20: Sample and Hold Conceptual Block .....	31
Figure 21: Sample and Hold Circuit for Red/IR PPG .....	32
Figure 22: Timing Circuit.....	33
Figure 23: Summing amplifier.....	34
Figure 24: Serial port to TCP/IP interface .....	37
Figure 25: PPG signal acquired from passive filtering.....	44
Figure 26: Filter response to motion artifact in PPG signal.....	45
Figure 27: Multilayered time-multiplexed signal .....	45
Figure 28: Time slicing in multiplexed signal .....	46
Figure 29: Impulses embedded in PPG showing detected peaks.....	47
Figure 30: Beat-to-beat heart rate calculations of commercial and project devices .....	48
Figure 31: Heart rate during exercise cycles.....	48
Figure 32: Blood Oxygen Saturation calculation results .....	49
Figure 33: Blood oxygen saturation during exercise cycles .....	50
Figure 34: PPG signal transducer .....	55
Figure 35: Prototype Circuit Board.....	55

## **NOMENCLATURE**

Blood oxygen saturation: Peripheral blood oxygen saturation, also known as SpO<sub>2</sub>

Heart Rate: As measured at the arteries, equivalent to pulse rate

Non-invasive: That which does not pierce the skin, nor does degrade the performance or integrity of the analyte and the areas which the analyte impacts (e.g., blood is an analyte and affects everything in the body).

NIHMS: Non-invasive Health Monitoring System



# 1 INTRODUCTION

People often find the need to track their personal health more efficiently, and monitor the status of another individual periodically and remotely. The health of a sick child at home or of a senior parent living overseas is of particular importance to people, especially when the situation becomes time critical. Periodic reports and immediate alerts for any sudden changes in their health may give people an opportunity to act quickly and save the life of the person in danger. Even from a personal health monitoring perspective, the ability to relay the health information collected to a doctor or to a hospital for advanced or emergency assessment would be a great asset to people.

## 1.1 Objectives

The aim of this project was to design and build a device, to be named NIHMS (Non-Invasive Health Monitoring System), which would provide users with a way to monitor various physiological indicators of their health. The device would be non-invasive in its measurements, and would be easy for the users to attach to themselves. In terms of its functionality, NIHMS would be capable of measuring multiple physiological signals simultaneously with good temporal resolution. The processing of these signals would be done on a computing device of user's choice, so as to utilize pre-existing processing power and displays. This would not only cut down on the cost of the product and make it more accessible to general public, but would also allow for NIHMS to be easily adapted into any existing infrastructure like home computers, portable laptops and smart cell phones. The device would also be able to integrate seamlessly into hospital networks to provide up to date information concerning the patients to the doctors on their PDAs. For such varied integration to be possible, NIHMS would be made to wirelessly transmit the measured signals to these processing centres, thus relying on a software integration protocol rather than a hardware one.

The health indicators that were chosen to be supported on NIHMS include the heart rate, blood oxygen saturation, blood pressure and breathing rate of the user among others, as they lent themselves to be measured non-invasively. The device would support these

indicators in a plug-and-play fashion. This would not only allow the user to customize their monitoring device, but would enable seamless future upgrades, where only a transducer for the new measurand and the software for processing it would be needed. This module of the project specifically deals with the design and implementation of the transducer to measure the signals necessary for blood oxygen saturation and heart rate, and the software implementation to process them.

## ***1.2 Scope and Methodology***

The scope of this module of the project deals with the measurement of blood oxygen saturation and heart rate of the user. It does not include the design of the device that would transmit the physiological signals necessary for these to a processing centre, which is the core component of NIHMS. However, the transducer and the software required to process the signals were designed in accordance with integration protocols of NIHMS and are considered part of the basic model of the NIHMS product.

The integration protocols of NIHMS required a transducer that was non-invasive in its method of signal acquisition from the user and produced a voltage a signal within the accepted range. The software was required to be as real-time as possible in its processing of the signal, requiring little to no storage of signal data in the processing centre's disk space. This was to ensure the portability of the software to processing devices with restricted storage space, for instance, smart cell phones.

Therefore, the methodology adopted for this module (hereon referred to as the project), was to use the non-invasive yet penetrative characteristics of light to acquire the necessary signals. Theory suggested that shining light through the tissue and observing the reflectance of light due to the arterial blood would allow for the characterization of blood flow dynamics and blood analyte composition. The signal thus acquired was converted to a voltage signal and scaled to be within the accepted range for NIHMS. After receiving this signal on the processing centre through NIHMS, it was processed in real-time to calculate the heart rate and the blood oxygen saturation of the user. In order to be as real-time as possible and be minimal in the usage of storage space, data pertaining to only a few seconds was collected and held in memory for processing.

## 2 LITERATURE REVIEW

Use of light to measure blood oxygen saturation and heart rate is called Pulse Oximetry, and is a field of study where abundant research has been done in the past few decades. Pulse Oximetry relies on measurement of a physiological signal called Photoplethysmography (PPG) [1], which is an optical measurement of the change in blood volume in the arteries. Pulse oximetry acquires PPG signals by irradiating two different wavelengths of light through the tissue, and compares the light absorption characteristics of blood under these wavelengths. The comparison leads to a measurement of the oxygenation of blood and is reported as blood oxygen saturation [1].

### 2.1 Transmittance vs. Reflectance

Pulse Oximetry has traditionally be done in two methods: transmittance and reflectance of light. In transmittance pulse oximetry, light is shone through the tissue using an LED and is detected on the other end using a photodiode. In contrast, reflectance pulse oximetry uses a photodiode on the same side as the LED to detect the light reflected by the tissue (Figure 1).

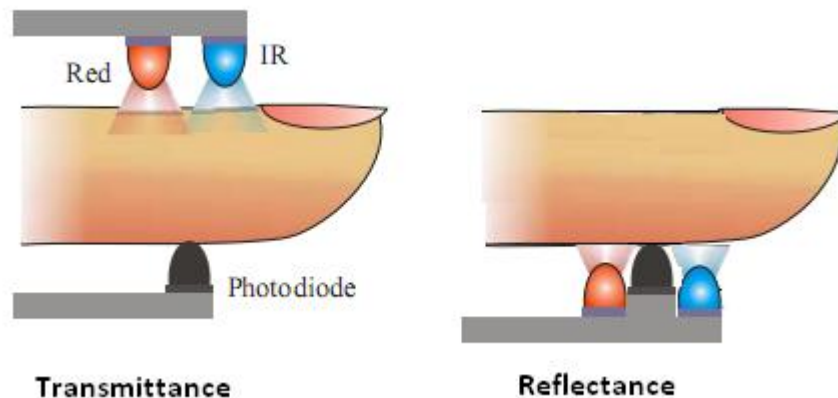


Figure 1: Transmittance and Reflectance configurations of transducer<sup>3</sup>

Although both the signals contain information pertaining to the changes in blood volume in the tissue, the relationship is not the same [8]. For instance, increasing the blood volume in the tissue decreases the light that is able to transmit through the tissue, but has

<sup>3</sup> <http://www.ph.surrey.ac.uk/~phs3ps/surj/v2/li.pdf>

the opposite affect on the reflected light. This can be intuitively justified, as the more blood there is in the tissue, the more the light passing through the tissue gets blocked. Since this improves the amount of light reflecting back, the signal observed in the reflectance configuration increases. Similarly, as the light gets blocked, not enough light reaches the photodetector in the transmittance configuration, and therefore a decline in the signal is observed.

In terms of the application, the transmittance configuration is more suited to the areas of the body that lend themselves better to light transmittance through them, e.g. fingers or ear lobes. However, transmittance configuration cannot be used in other areas of the body as the transmittance of light is significantly less when there are obstacles such as bones or muscle in the way, besides the fact that the path of light is much longer than in thin areas such as the ear lobes. In such scenarios, reflectance configuration is more useful, provided that vasculature is available close to the surface of the skin, e.g. forehead, wrist or forearm.

Reflectance configuration is not limited to areas where the transmittance configuration cannot be used. It can be employed to measure PPG signal from the ear lobes or the fingers just as the transmittance configuration. However, due to their thin cross-sectional area, fingers and ear lobes transmit much of the light shone through them, resulting in lower signal intensity in the reflectance configuration [8].

In further comparison, reflectance configuration is more susceptible to motion artifact than the transmittance configuration [7]. This is because transducers in transmittance configuration have the opportunity to distribute their weight around the cross-sectional area of the measuring space, as the photodetector is on the opposite plane as the LED. However, transducers in reflectance configuration are designed with both the photodetector and the LED on the same plane. This leaves them susceptible to movements due to their own weight and due to any motions of the user. However, provided that the transducer is secured properly to the measuring area of the body, motion artifact can be minimized.

## 2.2 Wavelengths of light

While such is the debate in the literature pertaining to the use of reflectance over transmittance configuration, essentially concluding that the choice depends on the demand of the task at hand, research for the choice of wavelengths of light mainly indicated the use of Red and Infrared wavelengths. Comparing light absorption characteristics of blood under Red and Infrared lights is said to provide a good basis for the measurement of blood oxygen saturation. Wavelengths of 660nm (Red) and 940nm (Infrared) were found to be most widely researched for this application [1][5], along with 890nm as an alternative Infrared wavelength [2].

The basis for using two different wavelengths of light is that oxygenated blood has different light absorption characteristics than deoxygenated blood. Thus, the two wavelengths are chosen such that the contrast between oxygenated and deoxygenated blood is sharply visible. In this respect, 940nm is a better choice than 890nm for a wavelength in the Infrared spectrum, as the contrast between oxygenated and deoxygenated blood is more accentuated at 940nm than at 890nm (Figure 2). Thus, when compared with the absorption due to 660nm light source for oxygen saturation calculation, the results will be less susceptible to noise.

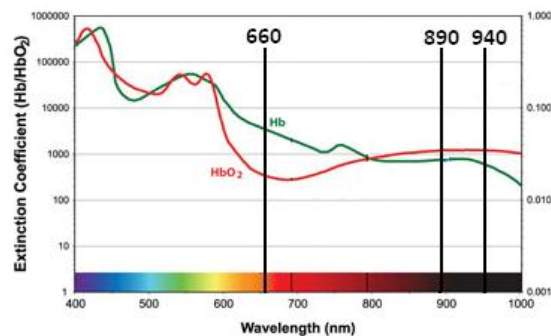


Figure 2: Light Absorption characteristics of HbO<sub>2</sub> and Hb at different wavelengths<sup>4</sup>

<sup>4</sup> [http://www.mandel.ca/products/Imaging/Pearl\\_Imager/Extinction\\_coefficient.jpg](http://www.mandel.ca/products/Imaging/Pearl_Imager/Extinction_coefficient.jpg)

### **3 PROBLEM STATEMENT AND METHODOLOGY OF SOLUTION**

This section will detail the theoretical basis of the project that helps in its aim to provide health rate and blood oxygen saturation measurements to the user of the product. The problem statement for the project will be defined and the methodology of the solution will be introduced.

#### **3.1 Theory of PPG and Heart Rate**

Photoplethysmography is a physiological signal measured to represent the flow of blood in the arteries. Heart pumps blood through the arteries of the body in a rhythmic fashion known as the cardiac cycle. The heart receives oxygenated blood from the pulmonary circulation into its left atrium as part of the atrial diastole. When the atria enter the systolic period, also known as the ventricular diastolic period, the left atrium pumps this blood into the left ventricle. During ventricular systole, the left ventricle contracts to push blood into the Aorta, the major artery supplying blood to the whole body. From here, the blood branches off into its various arteries carrying blood to all of the locations of the body.

This rhythmic flow of blood can be seen in decreasing degrees of clarity in arterial blood flow up until the level of capillaries. Though existent, the rhythmic flow is barely apparent after the blood crosses over into the venous return. Thus, it can be said that given a vascular bed the majority of the pulsatile blood flow is due to the arterial blood [1]. Thus, PPG wave predominantly represents the flow of blood in the arteries of the area being investigated.

PPG contains an abundance of information in its shape, height and timing. For instance, PPG is characterized by a second peak in each of its periods, which is called the “Dicrotic Notch” and represents the closure of the aortic valve after the end of systole, thus causing a backlash and a momentary increase in blood volume of the arteries [10]. The time period between each of the successive periods of the PPG waveform represents the repetition of the cardiac cycle, and thus can be used to calculate the heart rate. The peak

height of each of the PPG periods is affected by many things, including the blood pressure, the breathing rate of the subject, and the light absorption characteristics due to the composition of the blood, which is of most interest to this project in regards to the measurement of blood oxygen saturation.

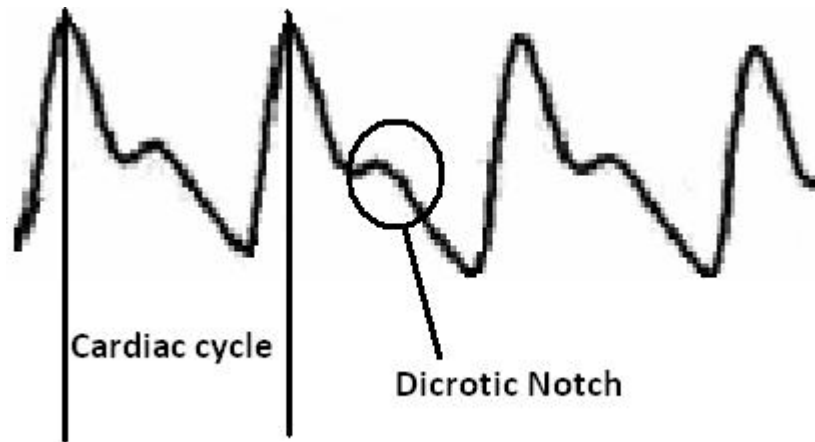


Figure 3: PPG waveform demonstrating blood dynamic features

### 3.2 Theory of Blood Oxygen Saturation

Blood is composed mainly of erythrocytes (Red blood cells), among other types of cells like leukocytes (white blood cells) and thrombocytes (platelets). Erythrocytes serve the purpose of carrying oxygen from the lungs to the rest of the body, and subsequently picking up carbon dioxide from the body for exhalation at the lungs. They accomplish this task through a molecule that is abundant in them called Haemoglobin.

Haemoglobin is a globular molecule, which is partly protein, with four iron ions ( $\text{Fe}^+$ ) acting as binding sites for oxygen and carbon dioxide molecules. These binding sites can bind other molecules like carbon monoxide and nitric oxide as well, but under normal circumstances, haemoglobin is used to carry oxygen in the blood. Haemoglobin is of particular interest to this project due to its changing light absorption characteristics based on its oxygen saturation level.

Haemoglobin's reflection of Red light increases as the number of oxygen molecules bound to it increases. Intuitively, this is a sensible trend as it is common to relate blood

that is bright red with oxygenated blood, and blood that is paler in color to deoxygenated blood. Theoretically, this trend takes its roots in the extinction coefficients of oxygenated and deoxygenated haemoglobin molecules. Extinction coefficient ( $\epsilon$ ) is a measure of the strength of absorbance for a molecule at a given light wavelength. The lower this value is, the better the molecule reflects the given wavelength. It is because this value is significantly different for oxyhaemoglobin and deoxyhaemoglobin at Red and Infrared wavelengths that calculation of blood oxygen saturation is possible. The extinction coefficients for them were found through research to be as follows [1]:

Extinction coefficient ( $\epsilon$ )	Oxyhaemoglobin (HbO <sub>2</sub> )	Deoxyhaemoglobin (Hb)
Red	0.81	0.08
Infrared	0.18	0.29

**Table 1: Extinction coefficient ( $\epsilon$ ) of haemoglobin**

Extinction coefficient thus governs the amount of light that is reflected back depending on the concentration of an analyte in the tissue. The relationship between the concentration of an analyte and the light intensity absorbed is called the Beer-Lambert Law [1]:

$$I_{out} = I_{in} e^{-cd \epsilon(\lambda)}$$

where  $I_{in}$  is the intensity of light originally shone at the tissue,  $c$  is the concentration of the analyte in the tissue,  $d$  is the path length of the light, and  $\epsilon(\lambda)$  is the extinction coefficient of the analyte at the wavelength of light shining through. Since there are two absorbers of light in this case, HbO<sub>2</sub> and Hb, the Beer-Lambert Law can be rewritten as follows:

$$I_{out} = I_{in} e^{-cd(S \epsilon_{Hb}(\lambda) + (1-S) \epsilon_{HbO_2}(\lambda))}$$

where  $S$  is the oxygen saturation (0-1).

Intensity of the original light and the light transmitting through after absorption can be measured independently of the concentration of haemoglobin and the path length electronically by measuring the current input to the LEDs and the current output of the



photodiode. A ratio R comparing the two intensities at Red and Infrared wavelengths, and two different instances of time can thus be written as,

$$R = \frac{\ln \left( \frac{I_{out}(t1)}{I_{in}(t2)} \right)_{Red}}{\ln \left( \frac{I_{out}(t1)}{I_{in}(t2)} \right)_{Infrared}}$$

Solving the rewritten Beer-Lambert law for oxygen saturation S in terms of this ratio and the extinction coefficients,

$$S = \frac{\epsilon_{Hb}(\lambda_R) - (\epsilon_{Hb}(\lambda_{IR}) \times R)}{\epsilon_{Hb}(\lambda_R) - \epsilon_{HbO2}(\lambda_R) + ([\epsilon_{HbO2}(\lambda_{IR}) - \epsilon_{Hb}(\lambda_{IR})] \times R)}$$

This relationship can now be used to calculate the oxygen saturation through measurement of ratio R, which can be done by comparing the IR PPG signal with the Red PPG signal.

### 3.3 Problem Statement

The task at hand for this project is to design and implement a transducer and the corresponding hardware for the measurement of Red and Infrared PPGs. The output of this system on the hardware side should be these two voltage signals, scaled to be within the accepted range of 0-5V for NIHMS. The requirement for reliable estimation of blood oxygen saturation is that these measurements be done at the same spatial location, and be done simultaneously. The reason for this is that if Red and Infrared PPGs are not acquired from the same spatial location, the blood being sampled is different and therefore cannot be assumed to exhibit the same absorption characteristics. This can possibly introduce significant error in the estimation of ratio R, and subsequently in the calculation of oxygen saturation. Similarly, if the two signals are not acquired simultaneously, because arterial blood is continuously flowing away, the signal acquired at the second time instant is again not from the same blood sample.

On the software side, the task is to receive these signals as a client of the NIHMS, and process them in real-time to produce heart rate and blood oxygen saturation measurements. The heart rate is required to be in the units of beats per minute, while the blood oxygen saturation should be a percentage value.

### *3.4 Methodology of Solution*

As established in the problem statement, calculation of blood oxygen saturation requires measurement of PPG waveforms using two wavelengths, Red and Infrared. Furthermore, the constraint that these two waveforms should be acquired in the same spatial location requires that only one photodiode be used, as using two independent photodiodes for Red and Infrared wavelengths would increase the size of the transducer. This would make it difficult to ensure that the location from which the PPG signals are acquired are the same. The photodiode therefore needs to be sensitive to a broad range of wavelengths in order to be able to acquire PPG signals from both the Red and the Infrared light spectrum.

The second constraint of ensuring the simultaneity of the acquisition of Red and Infrared PPG signals, and the design objective of using only one photodiode to do this, requires the use of a concept called Time Multiplexing. This involves alternating irradiation of Red and Infrared lights to share time on the photodiode channel for their respective acquisitions.

Since the photodiode inherently produces a current signal proportional to the light intensity it sees, a current-to-voltage converter that produces a voltage signal is required. Furthermore, the spectrum of the PPG signal has the most power in the range of 0.5 – 10 Hz [3]. Therefore the voltage signal needs to be filtered for range of the spectrum in order to extract the PPG signal.

Once the Red and the Infrared PPG signals are acquired, they will be input into the NIHMS data acquisition system to be wirelessly transmitted to the processing centre. Software running in the processing centre will be made to acquire these two PPG signals in parallel. The one PPG signal of the two that has a better signal to noise ratio will be used for the calculation of heart rate to ensure optimal accuracy. This will be done by measuring the time period between two consecutive periods of the PPG signal, thus providing a beat-to-beat heart rate calculation.

Since the voltage PPG signal is logarithmically proportional to the signal intensity, with the maximum intensity occurring during the peak of the systole and the minimum occurring when the blood volume is at its lowest in the arteries, the calculation of R can be rewritten in terms of the voltage as follows:

$$R = \frac{\frac{AC_{Red}}{DC_{Red}}}{\frac{AC_{Infrared}}{DC_{Infrared}}} = \frac{\frac{\max ( PPG )_{Red}}{\min ( PPG )_{Red}}}{\frac{\max ( PPG )_{Infrared}}{\min ( PPG )_{Infrared}}}$$

The maximum and minimum of the PPG signals will be thus be used to calculate the ratio R and the blood oxygen saturation.

## 4 DESIGN PROCEDURES

This section will present the design procedures that were implemented as per the methodology described in the previous section. The various hardware components that were used to acquire and extract the two PPG signals will be presented in detail, followed by the software infrastructure built for the purpose of parallel data processing on the processing centre. Finally, software data processing done to calculate the heart rate and the blood oxygen saturation will be presented.

### 4.1 LED circuits and Photodiode selection

First phase of circuitry that was implemented was very basic. In order to verify the sensitivity of the photodiode in Red and Infrared spectrums, a Red LED and an Infrared LED were connected to the function generator producing a square wave pulse at the frequency of 1 KHz. The photodiode (PNZ334<sup>5</sup>, peak sensitivity at 850nm, 75% at 660nm and 940nm) was directly linked to the positive and negative probes of the oscilloscope. Voltage level was zoomed into the range of 10mv/div to see the voltage signal being produced by the photodiode. The setup therefore is as shown in the figure below.

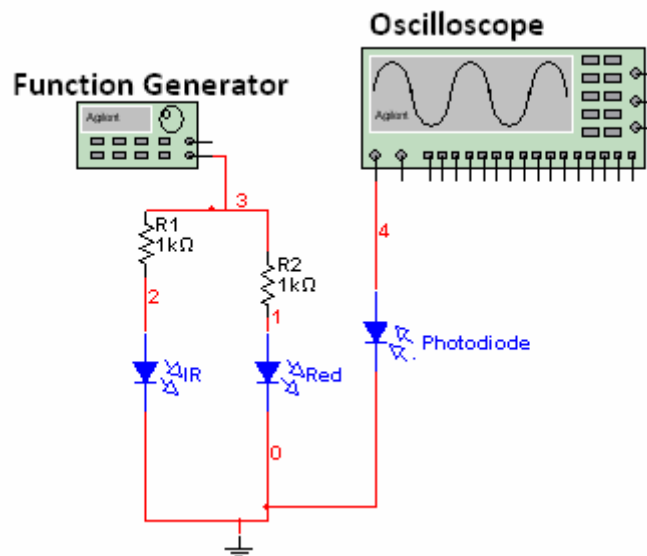


Figure 4: LED/Photodiode signal testing

<sup>5</sup> <http://www.media.mit.edu/resenv/classes/MAS836/PNZ334.pdf>

After such a setup, the photodiode was pointed at the LEDs individually to ensure that the square wave signal due to fast changing light intensity could be seen in the scope. This test accomplished two things: it first ensured that the photodiode was sensitive to both the Red and Infrared light, and it also ensured that the slew rate (the rate at which the photodiode is capable of changing between its extreme states) was enough to allow for capture of fast changing signals with good quality. Had this test failed, the photodiode would have been deemed insufficient for use in this project, as being the first point of signal acquisition in the circuit, it is absolutely crucial that the photodiode is sufficiently sensitive and fast enough to pick up both Red and Infrared PPG signals.

This test also provided an estimate of the signal levels that the light intensity produced in the photodiode, allowing for the design of subsequent circuitry of pre-amplification. It was found that the current that the Red and Infrared lights produced in the photodiode was in the range of a few nanoamperes, and required at least a gain of 10 million before it could be converted to a voltage signal in the range of volts.

## ***4.2 Current to Voltage Converter***

Once the photodiode was tested and was deemed to be sufficient for use in this project, the next step was to produce a voltage signal that was proportional to the light intensity produced by the LEDs. During the initial phases of implementation, it was thought that the photodiode produced a voltage signal by default and that a differential voltage signal from the two nodes of the photodiode needed to be acquired and amplified further. This misinterpretation of the signal seen on the scope during the testing phase delayed the implementation of a circuit to produce a voltage signal from the photodiode. Realizing that the photodiode produced a current signal and not a voltage signal, a current to voltage converter was implemented.

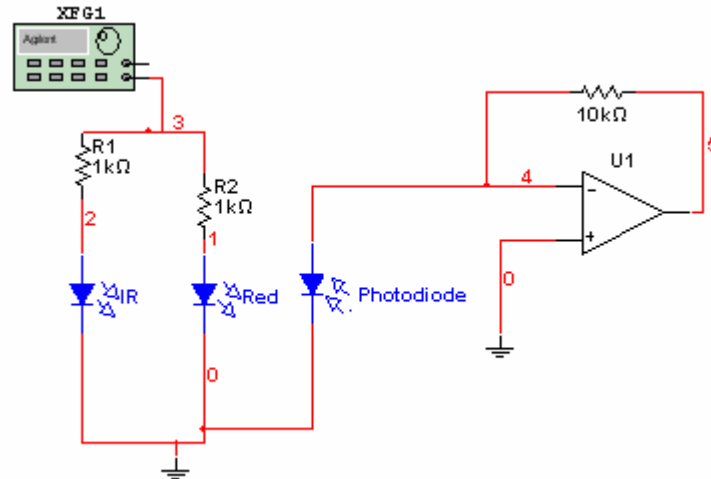


**Figure 5: Current to voltage converter**

Based on the rules of an ideal op-amp, it can be said that the input current to the negative terminal of the op-amp is zero. Therefore, any current that is produced due to the photodiode passes through the feedback resistor to the output. That is,

$$\frac{V_{-} - V_{out}}{R} = I_{in}$$

$$V_{out} = 0 - I_{in} R = - I_{in} R$$

Thus, the current signal produced by the photodiode was converted to a voltage signal at the output node of the op-amp, with a proportionality constant of  $R$ . Setting  $R=10k$ , the gain of the first stage was 10,000. Thus a current signal which was in the range of a few nanoamperes was then in the range of several hundred microvolts after this stage. The signal needed to be further amplified to be brought to the range of volts. However, it was deemed unwise to increase the feedback resistance of this stage to amplify the current signal further. This is because the gain of this stage was already high, and any further increase in gain would have deteriorated the signal in terms of its noise immunity. Furthermore, use of high values of resistance would not have been a good design decision, except if absolutely required, since the tolerance of 5% on a higher resistor value would mean a higher degree of fluctuations than for the same tolerance on a lower resistor value. It was decided that the use of resistors in the 100K – 1M range would be as little as possible through out the system to ensure smaller fluctuations.

The operational amplifier used in this circuit was a quad op-amp LM 324N. This was done to save space on the circuit board and keep things as close to each other as possible. In addition, this choice ensured that phases that worked towards accomplishing a common goal could be localized to a single IC, thus minimizing cross-board traffic and also ensuring consistency and circuit parameters such as gain and bandwidth for that phase.

### 4.3 Preamplifier

The previous stage of the circuit accomplished the task of converting the current signal produced by the photodiode into a voltage signal that was in the range of several hundred microvolts, which was still miniscule. Therefore, the next phase of the circuitry was designed to amplify the signal further before it could be filtered. It can be noted from the derivation of the voltage at the output node of the current-to-voltage converter that the voltage produced by it is in the inverted state. As the next few stages of signal processing are expected to produce more inversions of the signal, it was decided that there would be an inversion in this phase of the circuit to achieve proper polarity at the end. Thus, this phase became an inverting amplifier.

The decision to amplify the signal before filtering may seem odd considering that the next stage would suppress the power in the spectrum outside that of the range required for PPG. However, it was deemed necessary since the AC component of the signal was very small in comparison to the DC component. Filtering at this stage of the signal would not have suppressed the higher frequency noises in relation to the AC component of the signal very well. Therefore, the signal was put through further amplification before being filtered.

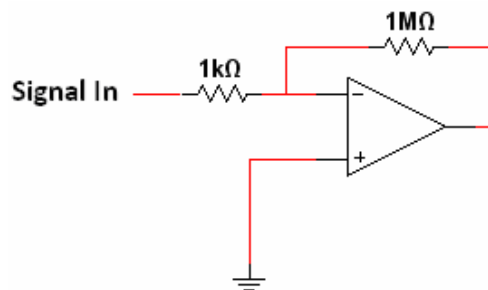


Figure 6: Inverting Preamplifier

This stage produces a voltage gain of  $(-1M/1K) = -1000$  on the input signal, bringing the voltage signal to the range of several hundred millivolts.

#### ***4.4 Signal Filtering***

The next stage of the circuit involves filtering the signal to remove various kinds of noises from it. These noises include the ever-present interference of the electromagnetic radiation from the power-lines in the form of a 60Hz sinusoid signal, and other such high frequency noises. Another important source of noise into the signal that was not realized before the design of the filter was the noise from the tube lights in the room. The light produced by tube lights flickers at a high rate, though it may not be visible to the human eye due to the fact that any change in the environment that is faster than 16 Hz is perceived to be more or less continuous. This flicker becomes a very large source of noise in the signal received from the photodiode, as the photodiode is sensitive to changes even as fast as 1KHz. Although the flicker that is directly produced by tube lights is around the range of 50-60Hz in its oscillations, the light is reflected off of various sources in the room, so much so that its noise spectrum becomes unpredictable.

Another source of noise in the signal is not due to ambient light, but due to the inherent features of the signal itself. The PPG signal is acquired by shining light at the vascular surface close to the surface of the skin and capturing the reflected light. However, before the light can reach the vascular bed and return to the photodiode, it needs to pass through various tissue constituents such as skin, fat, cartilage, bone etc., resulting in a constant DC offset to the signal. Since we are only interested in the AC component of the signal produced by the pulsatile arterial blood flow, this DC component can be considered a major noise source in the signal. Since this DC component is closely related to the tissue constituents, it can be very easily affected by the motion of the photodiode relative to the skin surface. Considered to be a motion artifact, it is very much possible that the photodiode may move during its use by the subject, causing significant changes in the DC component of the signal.

Research suggests that the spectral range of PPG is between 0.5 – 10 Hz [3]. Therefore a filter within this range was needed to extract out the PPG signal from the signal acquired



thus far. The initial choice during the testing phase was to build passive low pass and high pass filters, cascaded to form a band pass filter. The reason for this choice was to first and foremost confirm the presence of a reasonable PPG signal in the acquired signal using an easy circuit, and also for better control of the cut-off frequencies till this confirmation was achieved. Thus, the circuit built was as follows:

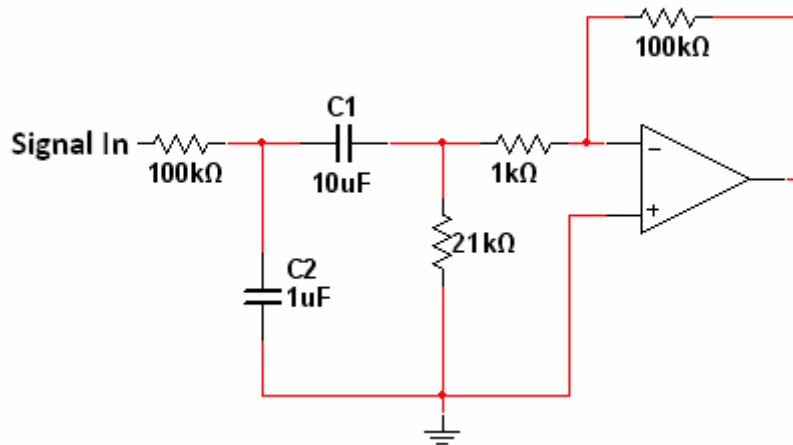


**Figure 7: Passive Band pass filter with Amplification**

The 3dB cut-off frequency of the low-pass and high-pass filters can be easily derived to be  $1/(RC)$ . Thus, the cut-off frequency of the low-pass filter was set to  $(1/(100k \times 1\mu \times 2\pi)) = 1.59$  Hz, Similarly, the cut-off frequency of the high-pass filter was set to  $(1/(21k \times 10\mu \times 2\pi)) = 0.76$  Hz

These cut-off frequencies were chosen since the roll-off of the first order filters is not very sharp (-20 dB) and therefore, higher frequency noise signals would not have been attenuated enough if not for such low cut-offs. However, it is clear from the choice of the cut-off frequencies that the DC offset would not be attenuated enough. Since this stage was built only on a temporary basis for the confirmation of existence of a PPG signal, further effort on improving this stage was not put in. With a gain of about 100 from the inverting amplifier stage attached to the output node of this band pass filter, this stage accomplished the task of extracting the PPG signal from the signal acquired thus far. Furthermore, due to its slow roll-off on the lower end of frequency spectrum, this stage

allowed the amplitude modulation of the PPG signal due to the breathing of the user to be clearly visible on the oscilloscope.

Though this modulation due to the breathing of the user is an attractive feature of the circuit, this entailed significant susceptibility of the PPG signal to motion artifact. There were many other such disadvantages to using a passive filter in this stage of circuit. For instance, the filter was very slow in reaching its steady state value, indicating that the poles of the circuit were very close to the origin of the s-plane. This meant that every time there was a motion artifact that disturbed the signal, the filter would take a long time settle back to the normal signal. In addition to this slow response, passive filters have a major drawback of being load dependant. In other words, the input resistance of the circuit to follow the filter had a significant impact on the cut-off frequencies of the filter. For instance, changing the amplification factor of the inverting amplifier at the output node changed the cut-off frequency of the low-pass filter, resulting in attenuation of the desired signal, or pass-through of undesirable noise spectrum into the output signal.

For these and many other such reasons, the practical choice of filter for the project was a second order active band pass filter. The criterion for building such a filter was a fast roll-off towards the DC frequency range, with an attenuation of about -40 dB at 1 mHz. The roll-off was designed to be equally sharp on the other side of the spectrum, but such that an attenuation of 0 dB was achieved around 10 Hz. Since the filter is active, the gain was set to be about 10. The design for a high quality band-pass filter was found during research<sup>6</sup>, whose transfer function was derived assuming identical capacitor values in the circuit. However, due to the lack of identical capacitors and due to the complexity of deriving the transfer function for different capacitor values in the circuit, the design was simulated in PSPICE till the required transfer characteristics were achieved with the capacitor values available. The design for such a filter is as shown in the following figure:

---

<sup>6</sup> <http://www.swarthmore.edu/NatSci/echeeve1/Ref/FilterBkgrnd/Filters.html>

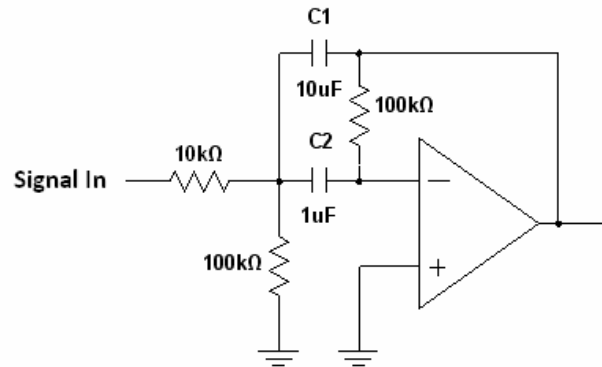


**Figure 8: Active Band-pass filter**

The transfer characteristics of the circuit above are as follows:

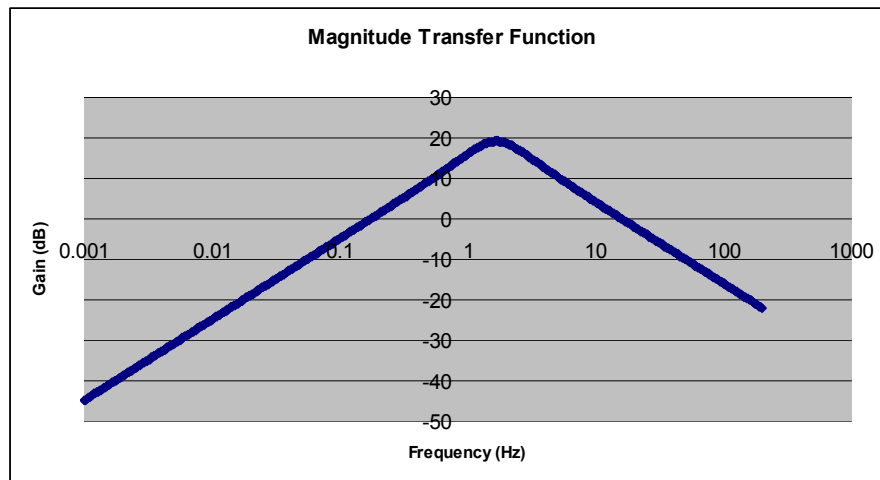


**Figure 9: Magnitude Transfer function of Active BPF**

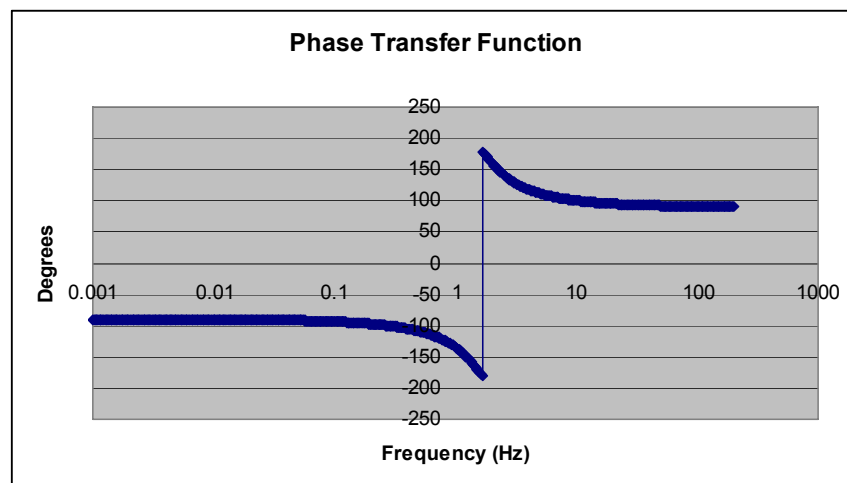


**Figure 10: Phase transfer function of Active BPF**

As it can be seen from the magnitude transfer function depicted in Figure 9, the centre frequency of the band pass filter is about 1.66 Hz with a gain of 20 dB. The roll-off of the lower-frequencies is very sharp with the gain reaching close to -40dB at 1 mHz, indicating that the DC component of the signal would experience significant attenuation relative to the centre frequency. The magnitude response reaches a gain of 0dB around 15 Hz, which can satisfactorily ensure the quality of the PPG signal. However, in practice it was found that the flickers due to the ambient light most usually oscillated at about 15 Hz, adding significant noise to the signal. This was remedied easily though by covering the transducer with an opaque cloth during signal acquisition.

It can be also seen in Figure 10 that the phase response of this filter is not linear indicating that there might be distortion in the output signal. Some frequencies experience a positive phase shift, while some experience a negative phase shift. However, in practice, the circuit did not seem to distort the signal very much. Although the smooth shape of a PPG waveform that was seen using the passive filter could not be achieved, the signal was still satisfactory and exhibited key features such as the dicrotic notch properly.

#### ***4.5 Time Multiplexing***

Acquisition of a stable PPG waveform was a significant milestone in the progress of the project. The task that was remaining was to acquire two PPG signals simultaneously. Since one was already acquired, simultaneous acquisition seemed only to be a simple augmentation of the circuitry. However, there were many challenges to accomplishing the simultaneity of the acquisition.

Before the challenges faced can be discussed, introduction of the concept of time multiplexing is necessary. Time multiplexing in hardware is in some ways analogous to the concept of multithreading in software. Multithreading is a way to execute multiple threads of software code simultaneously, or the simulation of it. Most computers in the yesteryear had single core processors that could only execute one instruction at a time, albeit at an amazing speed, at the edge of every new clock pulse. In order to allow a scenario where one thread of software code does not have to wait for the current thread of code to finish execution for its own execution to begin, processors could be instructed to

alternate execution between the two threads. In other words, given threads A and B, and the requirement that neither thread should need to wait for the other to complete, the processor would execute an instruction from thread A, switch to the execution of an instruction from thread B for the next clock cycle, and then switch back to thread A. This process would repeat at a speed determined by the clocking frequency, also known as the speed of the processor. Since this alternation of thread execution is very fast, it creates an illusion of simultaneity where both threads A and B seem to be executing at the same time on a single core processor. This can be depicted easily in a picture as shown in the following figure.



**Figure 11: Multithreading**

Admittedly, this is a very simplistic view of the multithreading, as the real-world implementation involves various algorithms to prioritize and schedule thread execution in the processor. Even from this simplistic view, it is evident that if only one of the threads had been executing on the processor for all time cycles, the frequency of execution of each of the instructions in that thread is the same as that of clock frequency. However, in a multithreaded scenario, multiple threads share time on the processor, and therefore, their execution speed is not the same as when they were being executed exclusively. An interesting point to note is that the time that each of these threads gets allocated on the processor is an integer factor of the clocking frequency. This can be best explained using a picture as shown below, where it is clear that the duty cycle of the processor dedicated to thread A is half that of the normal duty cycle, as is the frequency of the cycle.

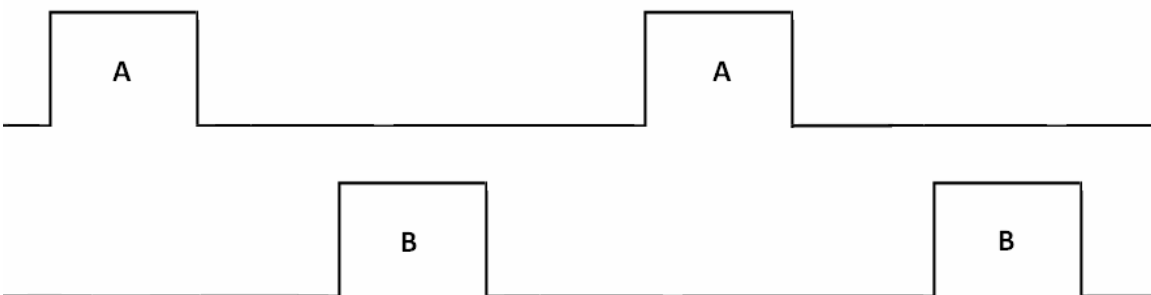


**Figure 12: Time sharing affects of Multithreading**

Time multiplexing in hardware is similar to the concept of multithreading. It is employed to make use of a single channel to transmit and receive multiple signals simultaneously. As with multithreading, this is done by sharing the time available on the channel between all of the signals that need to be transmitted. Furthermore, just as the execution speed of the threads reduced due to the need to share the time available on the processor with competing threads, the more signals there are that need to be transmitted using the channel, the lower the quality of each of the signal that is received on the other end of the channel. Fortunately, this reduction in quality does not become too apparent until the time slice available to each of the signals becomes too sparse due to too many competing signals. The quality of the signals received can be improved by taking advantage of the spectrum of the signals, or by increasing the clocking frequency of the channel being used in order to create more time slices.

The essential concept of time multiplexing revolves around the fact that simply transmitting the signals all at once through the channel is troublesome due to cross-contamination of the signals while they are within the channel. It is very a tedious task to predict how each of the signals will contaminate the others, and is definitely an even harder task to deconvolve each of the signals on the received end of the channel. Thus, the major goal in time multiplexing is to ensure mutual exclusivity of each of the signals in time, which allows transmittance of signals without cross-contamination through the channel. It also provides an easy way to deconvolve the signals on the receiving end provided that the receiver knows when to expect each of the signals.

Construction of a time multiplexed signal is done by sampling each of the signals at specific time instances. Each of the signals is allotted a time slice, just as with threads in multithreading, and their amplitude value at the repetitions of these time slices are noted down<sup>7</sup>. Thus, the time multiplexed signal assumes the values of these signals at time instances allotted to each signal. This can be shown pictorially as in the figure below.

---

<sup>7</sup> [http://en.wikipedia.org/wiki/Time\\_multiplexing](http://en.wikipedia.org/wiki/Time_multiplexing)

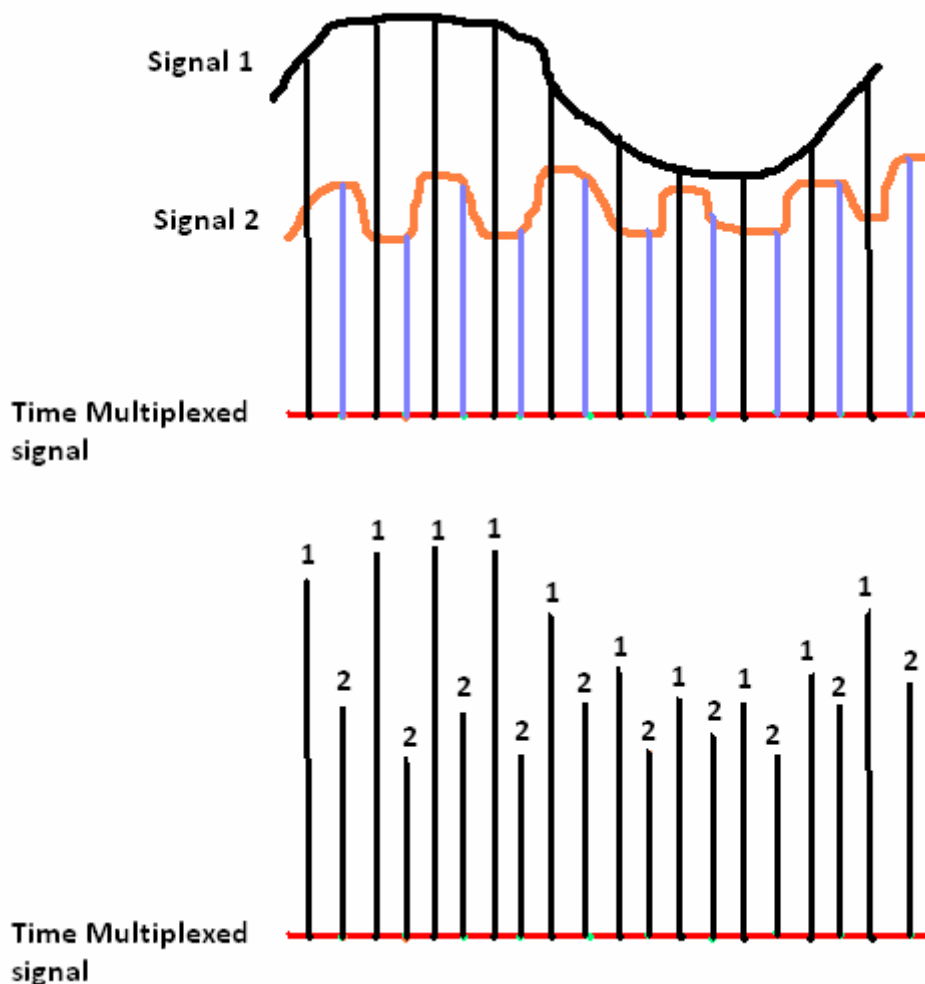


**Figure 13: Sampling of signals in Time Multiplexing**

As it can be seen in the above figure, the time multiplexed signal is an impulse train whose amplitude is modulated by each of the signals at specific time instances. Thus, if the receiver knew the association of the impulses in the time multiplexed signal to each of the signals, it can easily deconvolve them by simply sampling the time multiplexed signal at the right instant of time.

While this is helpful in understanding the concept of time multiplexing, it should be understood that impulse trains for sampling cannot be implemented in hardware easily. Instead, short duration square pulses are used as the closest alternative. Similar to the modified clock signals that result from time slicing in multithreading, a square wave

pulse whose duty cycle is less than 50% is used to sample and modulate each of the signals. Duty cycle of this control signal needs to be less than 50% to ensure mutual exclusivity of time slices allotted to each of the signals. If the duty cycle was more than 50%, then the time slice of one signal would overlap with that of the others and would give rise to cross-contamination while in the channel. Although the duty cycle of exactly 50% still guarantees mutual exclusivity theoretically, it is difficult to ensure that the square pulses have a duty cycle of exactly 50% and do not experience any phase shift over time. Therefore, in order to ensure the robustness of mutual exclusivity, the duty cycle is set to be moderately less than 50%.

In addition to controlling the duty cycle of the control signal to ensure the quality of the signals on the receiving end, the frequency of the control signal needs to be chosen efficiently too. As shown in Figure 13, the signal which varied slowly corresponding to the frequency at which it was sampled was captured better in the time multiplexed signal allowing for better reconstruction on the receiving end. However, if the signal changes too much between the sampling periods, much like the second signal, the changes get lost in the sampled signal and cannot be reconstructed reliably on the receiving end. This classic problem in sampling of signals is known as aliasing<sup>8</sup>. Therefore, to ensure that the fast changes in the signal are captured properly, the sampling frequency needs to be many times higher than the highest frequency component in the signal being sampled as per the Nyquist criterion.

Considering the single photodiode as the channel that needs to be time multiplexed, and the IR and Red PPG waveforms as the signals that need to simultaneously pass through this channel, the proposal for implementation was to time multiplex IR and Red PPGs through the photodiode and deconvolve them on the other end through sample and hold circuits. In other words, IR and Red LEDs would be irradiated only within their given time slices, and the response from the photodiode would be sampled and held at precisely these time instances for each of the PPG signals. The control signals for the sample and hold circuits are therefore the same signals as being used for time multiplexing.

---

<sup>8</sup> <http://en.wikipedia.org/wiki/Aliasing>



#### 4.6 555/556 Timer

The first ingredient needed in the construction of a time multiplexing control signal is a clock signal that can be thought of as an incremental step between the states of time multiplexing. For each clock period, the timing circuits enter a state of whether to irradiate the IR LED, or the Red LED, or neither of them. The duty cycle of this clock signal was chosen to be 50% and the frequency was chosen to be 1.1 KHz, which is significantly higher than the highest frequency component present in the PPG signals (10~15Hz) and ensures that there will be no aliasing problems in the sampling process.

One of the methods considered for generating such a clock signal was by the means of an oscillator. A Wein-bridge oscillator could be used to generate a 1.1 KHz sine wave that could be put through a Schmitt Trigger to produce a 1.1 KHz square wave. However, such a circuit was deemed slightly unstable considering that Wein-bridge oscillators are difficult to start up and Schmitt Trigger may produce unexpected changes in the clock signal due to noise contamination. The second alternative available to generating a consistent clock signal was through 555 Timers. 555 Timers are ICs specifically used to produce clock signals with great precision and allow customization of the frequency and the duty cycle of the clock signal.

Much like the initially proposed idea of using an oscillator coupled with Schmitt Triggers, 555 timers have two comparators within them that compare an input signal to a threshold value and trigger a change of state in the output signal. Using 555 timers to generate a clock signal involves exploiting this trigger mechanism to setup states that once again set off the trigger, resulting in a repeated change of state. The timer uses the charging and discharging cycle of a capacitor to control the frequency and the duty cycle of the clock pulse that is generated. This is because the rate at which the capacitor charges to its steady state voltage and discharges to its minimum voltage, known as the time constant, is very well understood and customizable. This time constant is governed by the capacitance value of the capacitor and the resistance in its charging or discharging circuit, and is given as  $\tau = R \cdot C$ .

If the input voltage is set to be the voltage that built up on the capacitor, and the threshold is set to be the voltage on the capacitor after time  $\tau$  (time constant), then the higher comparator of the 555 timer is triggered  $\tau$  seconds after the capacitor begins to charge up, as the input voltage would have reached the threshold voltage precisely at that moment. By cleverly setting up the circuit such that the change of state of the timer stops the capacitor from charging further and creates a discharge path, the timer can be reset by having the input signal reach the threshold of the lower comparator. Thus, as the capacitor oscillates between the two thresholds of the higher and lower comparators, the output of the timer oscillates between hi and lo states. Furthermore, by having different resistance paths for charging and discharging cycles, it is possible to change the duty cycle of the output clock signal, as the capacitor spends different amount of time in either of the states.

The timer was thus designed to produce a 1.1 KHz clock signal with a 50% duty cycle, and the circuit for this is as shown in the following figure:

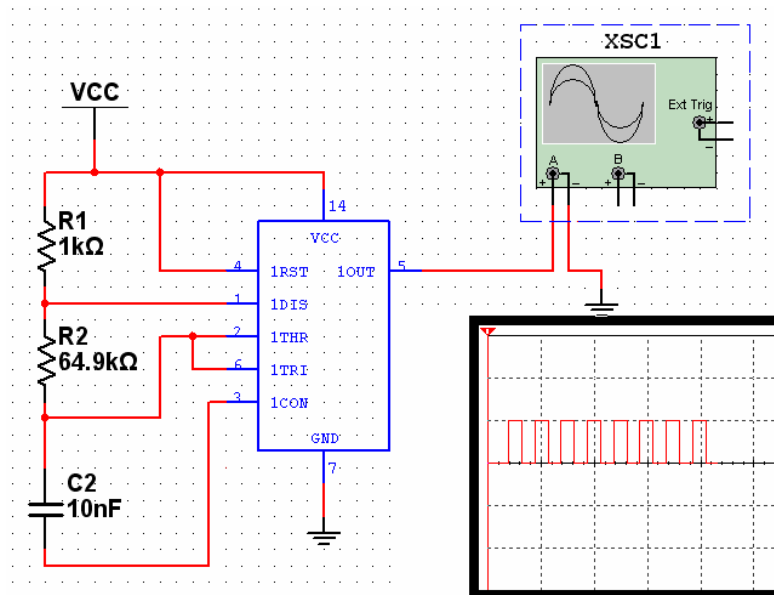


**Figure 14: 555/556 Timer circuit generating 1.1KHz clock signal**

For the purposes of the project, 556 timer was used to generate the clock signal. 556 timer is a dual timer IC and essentially contains two 555 timers within it. This was only done as a prospective measure for the possibility of needing two different clock signals.

However, in the final prototype, only one clock signal was needed, and therefore a 555 timer could have very well been used instead.

#### 4.7 Decade Counter

With the construction of a clock signal, the next step was to design a state system that would output the time multiplexing control signals. The three states that were needed for a clean time multiplexed signal without cross-contamination of the signals therein were:

Red LED on, IR LED off

Red LED off, IR LED on

Both LEDs off

The need for the third state where both the LEDs are off was to ensure that the duty cycle of other two states was less than 50% and to allow for a relaxing period for the photodiode and the LEDs. If the first two states were very close to each other in their timing, and the slew rate of the photodiode was not fast enough to change states correspondingly, there would be an overlap of states in the channel creating cross-contamination. Thus, the third state was introduced as a period where the signals from two earlier states could settle down satisfactorily.

The iteration of the state machine through these states is straight-forward: visit the first two states described above repeatedly by interleaving state 3 in between these states. This can be shown pictorially as follows:

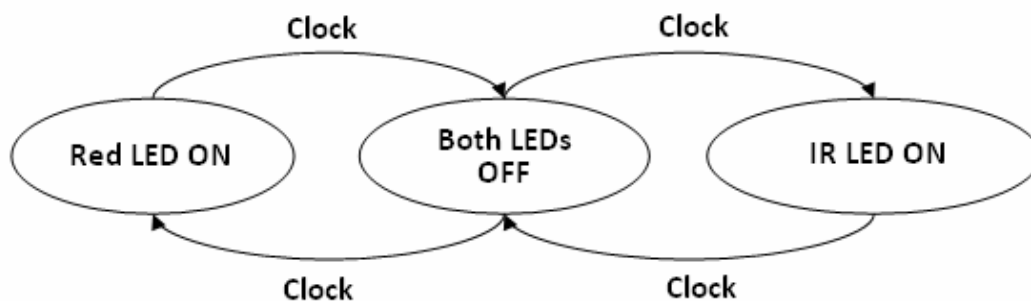


**Figure 15: State machine of Time Multiplexing**

Although this may seem logical at first and this is the fashion in which the state machine needs to function in the end, it can be easily noticed in Figure 15 that the interleaved state

of “Both LEDs OFF” is ambiguous in terms of its state change direction. When in this state, whether the state machine should change to the “Red LED ON” state or the “IR LED ON” state depends on which state the machine was in previously. Therefore, in order to make this fact clear and remove the ambiguity of the state direction, the state machine can be better represented as in the following figure.

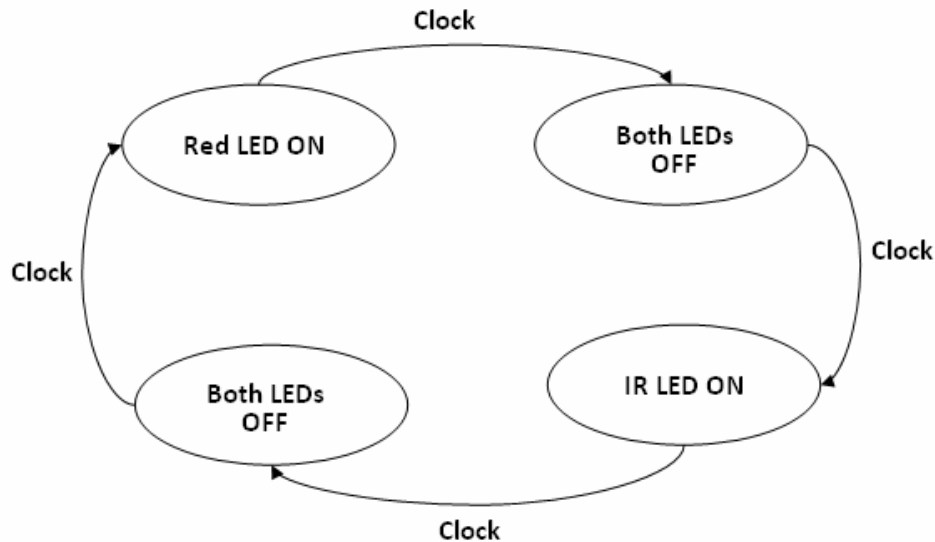


**Figure 16: Improved state machine for Time Multiplexing**

Implementation of state machines in general is a difficult task as the process usually involves various decision making steps in choosing which state to transition into. Fortunately, however, the state machine required for time multiplexing is much simpler, as shown in Figure 16, as there are no decisions to be made in the transition of states. The machine simply transitions from one state to the next upon every clock cycle. Perhaps the only intelligence needed in this state machine is for it to realize to reset to state 1 after reaching state 4, as there is no state 5 to transition into. If a closer look is taken of this state machine, it is not hard to realize that this is in fact identical to the state machine of a counter. A counter counts up from a base number to its maximum value, and if instructed to do so, resets to its base number to begin counting up again. Thus, implementing a counter in hardware is equivalent to building this state machine.

A Decade counter (HCF4017BE) was exactly the device needed for this purpose, and was therefore chosen to implement this state machine. A Decade counter counts up in decimal

format from 1 to 10, and the last state can be made to trigger a reset switch that brings the counter back to 1 on the next clock cycle. For each of the numbers, there exists an output pin on the IC, which when viewed from the perspective of time multiplexing, can be considered as the control signal output for each time slice. Only one of these pins is in hi state at any given point in time, making mutual exclusivity an inherent feature of the Decade Counter. Furthermore, since the duration of any of these state is the same as the duration of the clock cycle, and since the state machine repeats itself every 10 clock cycles, the duty cycle and the frequency of these states are  $1/10^{\text{th}}$  of that of the clock signal (i.e., 110 Hz and 10% duty cycle). The control signals thus generated by a Decade Counter look as shown in the following figure.

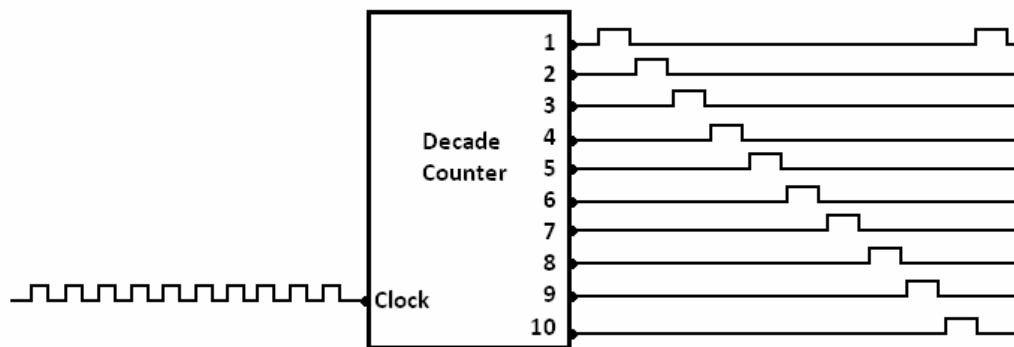


**Figure 17: Signal output from Decade Counter**

In order to implement the state machine needed for time multiplexing, the various states of the Decade Counter were categorized into the states of time multiplexing state machine. State 5 of the Decade Counter was chosen as the “Red LED ON” state, and state 9 was chosen as the “Infrared LED ON” state. The remaining states were categorized as “Both LEDs off” state. The reason for choosing state 5 as the beginning point of the time multiplexing state machine is that this allows for a settling period before the sampling process begins once the circuit is powered up. Any power-up transients that exist when the sampling circuit is powered on are expected to settle down while the Decade Counter is counting up to reach state 5. Thus, the state machine of the time multiplexer can be represented by that of Decade Counter as follows:

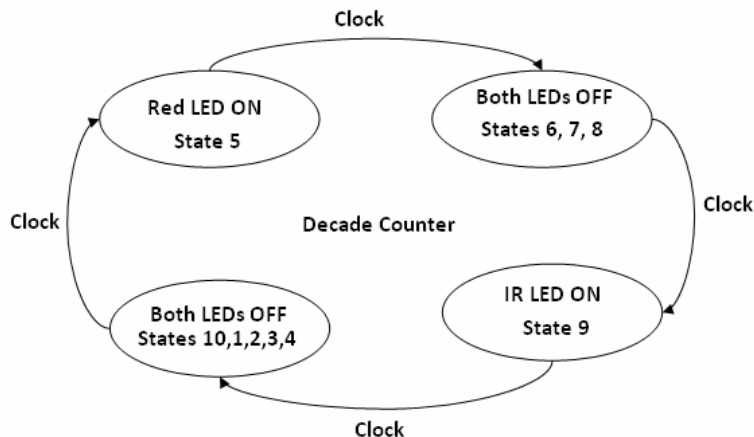


**Figure 18: Decade Counter state machine for Time Multiplexing**

This state machine may look like it is imbalanced with respect to “Both LEDs OFF” state, as the first of these states runs for three numbers, while the second one runs for five numbers. This is in fact true, and an ideal state machine would have had equal amount of numbers assigned to both these states. However, owing to technical difficulties where the Decade Counter would not reset for any control signal except the one that came from state 10, the state machine had to be implemented as so. This is not a problematic scenario by any means except for the possibility that the sampled Red PPG signal may decay more than the IR PPG signal while it is being held, as there is more delay between consecutive samples in Red PPG’s case. However, since the decay rate of the holding capacitor was much lower than the sampling rate, this did not cause any signal distortions. The final circuit that was implemented for the construction of time multiplexing control signals using Decade Counter is as shown in the following picture.

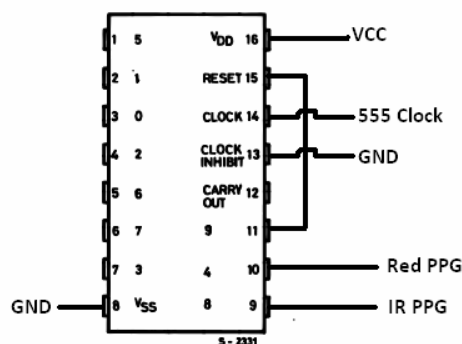


**Figure 19: Decade Counter Circuit<sup>9</sup>**

<sup>9</sup> <http://www.datasheetarchive.com/download/?url=http%3A%2F%2Fwww.datasheetarchive.com%2Fpdf-datasheets%2Fdatasheets-20%2FDSA-391685.pdf>

### 4.8 Sample and Hold Circuits

Completion of the 555/556 Timer and the Decade Counter circuits meant that a successfully time multiplexed signal could be sent through the photodiode channel. The next step was to receive this time multiplexed signal and deconvolve the two signals from it. It is to be noted that the time multiplexed signal is a square wave modulated and time sliced signal, whose amplitude is modulated by the sampled signals. Thus, the deconvolution process involves detecting the envelope of this signal at specific time instances. As mentioned in §4.5, this was done using sample and hold circuits. Sample and hold circuit blocks serve the purpose of sampling an incoming signal at specific instants of time, and holding the sample in memory till they are instructed to sample again. Thus, keeping track of the samples stored in the memory results in a signal that is a sampled version of the original incoming signal. Conceptually, the sampling circuit block can be represented as follows:

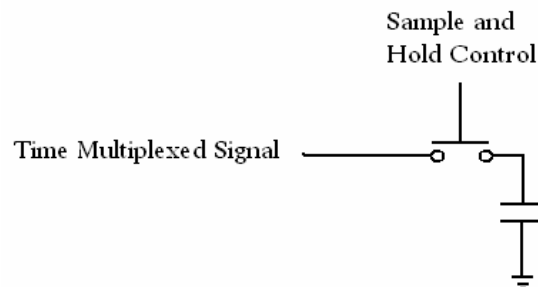


**Figure 20: Sample and Hold Conceptual Block**

In order to deconvolve signal A from the time multiplexed signal, the Sample and Hold circuit block needs to sample this signal at exactly the same instant of time as when signal A's sample exists in the time multiplexed signal. There would have been synchronization issues between the sampling and hold block and the time multiplexed signal had there been a need for the sampling and hold block to construct its own control signal. However, since the control signals for time multiplexing are available from the previous phase, they can be directly employed in this phase, thus resulting in perfect synchronization. The control signals for time multiplexing place a sample of one of the signals in the time multiplexed signal and also ensure that this sample is held by the sample and hold block at the same time.

Sample and Hold circuits were implemented using LF398N, which is an IC specifically designed for this purpose. An important thing to note about this IC is that it operates only within a certain range of input voltages. Thus the time multiplexed signal needed to be within a voltage range of -1 V to 1V to ensure reliable sampling. This was partly a reason for the choice of gain of the Preamplifier circuit (§4.3). The choice of the capacitor used in the circuit is also significant as it governs both the acquisition time of the signal and the decay process of the held signal. Choosing a large capacitor resulted in very slow decay process, but impacted on the acquisition time. However, choosing a small capacitor resulted in the quick decay of the held value. The value of 1 $\mu$ F for the capacitor was thus chosen based on experimental analysis, and was found to be good in both its acquisition time and its decay process for the purposes of this project. Two sample and hold circuits were implemented to capture the Red and IR PPG signals from the time multiplexed signal as follows:

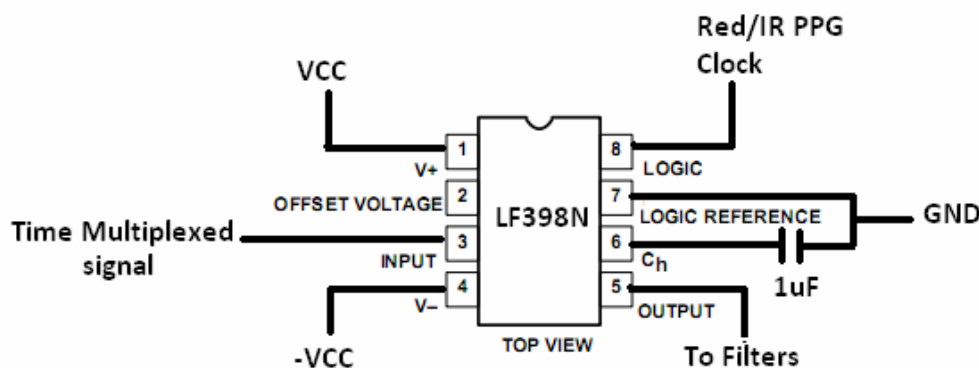


Figure 21: Sample and Hold Circuit for Red/IR PPG<sup>10</sup>

Once the signals had been captured by the sample and hold blocks, they were each sent to their respective filters (§4.4) to extract out the PPG waveforms. These waveforms will be end results of the hardware part of the project, and will be sent to the data acquisition device to be transmitted to the processing centre.

#### 4.9 Timing Circuit

When the 555/556 Timer, Decade Counter, and the Sample and Hold circuits are put together, they can be classified as being part of the Timing circuit. Another important

<sup>10</sup> <http://www.datasheetcatalog.org/datasheet/philips/LF398D.pdf>



piece of hardware that employed the control signals from the timing circuit for irradiating IR and Red LEDs was the Bilateral Switch IC. Not only can the LEDs draw sufficient power from the control signals, but they also degrade the control signals significantly. In practice, it was observed that the LEDs dropped the control signal voltage significantly enough that the signals could not trigger the sample and hold blocks anymore. For this reason, the LEDs were made to acquire power from  $V_{cc}$  instead, and were controlled using the Bilateral Switch IC (CD4066BE). This figure shows the Timing circuit in its entirety, including the Bilateral Switch.

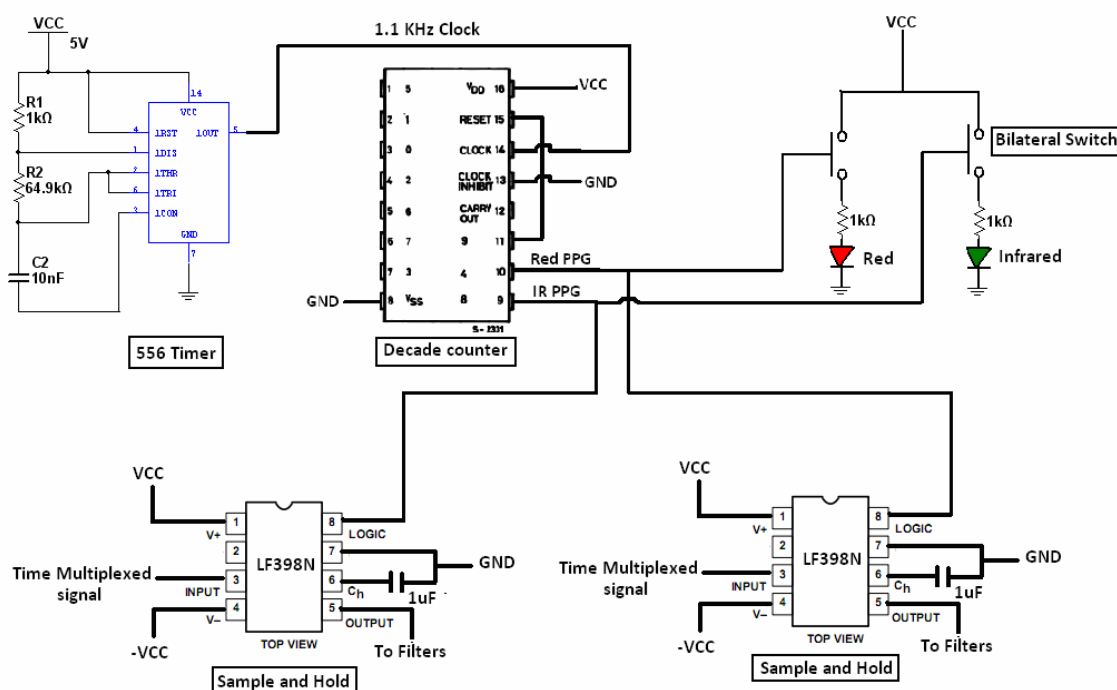
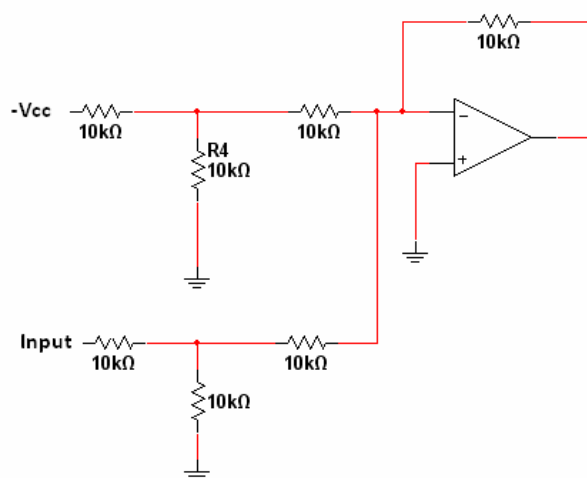


Figure 22: Timing Circuit

#### 4.10 Summing Amplifier

Once the signals are processed and cleaned, in order for them to be fed into the NIHMS data acquisition system, they need to be within the voltage range of 0-5V. Since the DC offset is actively removed from the PPG signal during signal processing, it varies between  $+V_{cc}$  and  $-V_{cc}$  volts. Assuming  $V_{cc}$  is always less than or equal to 5V, the signal needs to be scaled and moved into the region of 0- $V_{cc}$  volts. In other words, for a given signal  $X$ , the processing needed is  $Y = 0.5X + 0.5V_{cc}$ . The implementation procedure for this involves a summing amplifier which takes in the scaled versions of

these signals and adds them. Since the summing amplifier inverts the signal, the polarity of the signal was made sure to be already inverted in the previous phases. Furthermore, the offset to the summing amplifier was set to  $-0.5V_{cc}$  to ensure that the signal was in the range of 0 to  $V_{cc}$ , not  $-V_{cc}$  to 0 after the summing amplifier. Two separate summing amplifiers were used for Red and Infrared PPGs. Thus, the signal at the end of this circuit was ready to be input into the NIHMS data acquisition system.



**Figure 23: Summing amplifier**

#### **4.11 Serial Port to TCP/IP interface**

Conversion of the analog PPG signals into digital domain and transmittance of these values via Bluetooth to the processing centre is out of the scope of this project. However, since the project includes software that processes this data upon reception, the author sees it necessary to describe the infrastructure deployed in the processing centre to receive the data being transmitted.

The data is received on the processing centre using a Bluetooth adapter that plugs in via the USB port, if the processing centre is a computer. If the processing centre is another device such as a smart cell phone, it is assumed that the device already is, or is made capable of, receiving data via the Bluetooth. A generic Bluetooth adapter chosen for the purposes of this project appeared as virtual COM port on the computer after its successful installation. Once the device found the broadcasting Bluetooth connection of the NIHMS data acquisition system, it was paired and authorized for automated connection with the

device. This allowed for seamless integration of the software side with the NIHMS hardware.

Since the adapter appeared as a virtual COM port device on the computer, the data being broadcasted by NIHMS could be easily received by simply opening a serial port communication channel with this COM port and reading a predefined number of bytes of data from it. The software language chosen for this purpose was Ruby along with Win32Serial extension module<sup>11</sup>. Ruby code was easy to write and being an interpreted language, it could be easily ported to any platform that supported it, allowing for greater adaptability as was promised by NIHMS.

It was agreed with the NIHMS data acquisition system that the data being transmitted would be in the following format: “B<Channel1>;<Channel2>;< Channel3>;< Channel4>...”. Each of data packets in this serialized package is a digital value of one of the signals being read by data acquisition system. For instance, Red PPG and Infrared PPG signals could take up Channel1 and Channel2 slots in the package. Also, prefixing the package with the character “B” to signify a beginning or a break point allowed the processing centre to tune into the data acquisition system at any point during the transmission and recognize a new and complete package of data that was coming in. If the prefix was not present, the processing centre would not have been able to identify each of the channels individually. Furthermore, each of the channels was agreed to be 4 characters long and would represent a voltage value in the range of 0 to 5000 millivolts (i.e, 0000 – 5000). Thus, allowing the receiving system to know how many channels to expect in a given package beforehand, it was possible to make it read (5 \* # of channels) bytes from the serial stream after the detection of “B” character (5 characters per data point, including “;”). The receiver could very well have been implemented to read from the serial stream and deduce the number of channels dynamically. However, this was not done in order to keep the receiver simple.

---

<sup>11</sup> <http://grub.ath.cx/win32serial/>

Receiving data from the serial port resulted in richly sampled data stream for each of the channels being transmitted. However, due to the nature of serial port reading, it could only have been opened by any one program to process the data. Since the various channels in the data package represented different signals being acquired, a single application to process them would not have been logistically efficient. Furthermore, one of the features of NIHMS was to make this data available to any client upon request. Thus, it was determined that a TCP/IP server would be setup on the processing centre that would read the data in from the serial port and distribute to any interested clients connecting to it. This meant that multiple applications could run in parallel to process each of the signals independently. In addition to this, there was no longer a constraint that the application should be running on the processing centre. Since the data was available on TCP/IP, any remote computer or smart device could connect to the processing centre, receive the signal of its choice and process it locally, allowing for a significant increase in processing power allotted to signal processing.

Therefore, a multithreaded TCP/IP server was written with a main thread, whose purpose was to read incoming data from the serial port. A worker thread was started to open a TCP/IP port to listen and wait for connecting clients. Once a client connected to the server, the worker thread spawned a slave thread for that client. One of the first thing that each of the slave threads did was to wait for the client to respond with an identity value indicating their choice of channel. Once this value was received, the slave thread picked up the corresponding channel value from the data being read by the main thread and sent it to the client. This process was continued till the client either chose to end the connection or dropped the connection inadvertently. The slave thread then logged a closed connection and expired.

Though this design of the TCP server was expected to work well when implemented, due to inherent limitations in Ruby's ability to handle threads, the throughput of the server suffered significantly. A thread executing a system call operation on the computer would block all other threads in Ruby till that operation completed. Since, reading from a serial port is considered a system call operation, and since this was the most important of all

operations in the TCP server, all slave threads dealing with the clients were blocked and starved of CPU time. This resulted in a very slow transmission of data to the clients (1-2 samples per second) and essentially made the application useless.

The remedies that were considered for this problem included rewriting all of the application in another, more robust, language such as Perl or C. However, the option chosen for the sake of simplicity was to decouple serial port reading and TCP/IP transmission into two different Ruby applications. This meant that the serial port reading would no longer be considered a blocking operation in the TCP/IP server allowing for the operating system to decide on thread prioritizing instead of Ruby engine. A separate application was written to read in serial port data, connect to the TCP/IP server as a client, and supply its data to it, all as part of a single thread. On the side of the TCP/IP server, an additional port was opened specifically for the serial port reader to connect to. This can be represented conceptually as in the figure below.

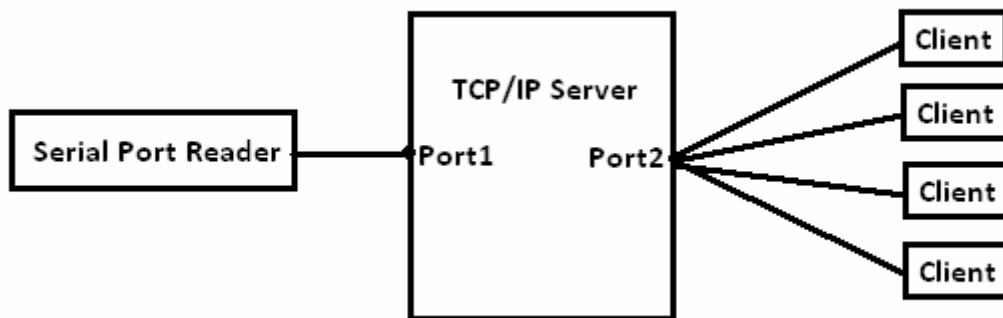


**Figure 24: Serial port to TCP/IP interface**

Although this significantly improved the throughput of the system, the richness of the data received by the clients was not the same as that was being seen by the serial port reader. This could be attributed to both Ruby's speed in handling multiple threads, and the fact that the clients were now reading data in a fashion similar to the tickertape system. If the clients were too slow to request the data from the TCP/IP server, or if slave threads in the TCP/IP server was too slow to fetch data from the main thread, then several sample points that were read from the serial port in the mean time would have become obsolete. This resulted in a significant portion of sample points never reaching the clients,

thus having clients receiving under-sampled signals. However, these limitations could have been easily fixed by migrating to a more powerful software language like C.

#### ***4.12 Heart Rate Calculation***

Once the data was received in a digital format on the processing centre, it could be easily imported into processing software such as MATLAB to calculate the necessary biometrics. Heart Rate calculation was done on the Red PPG signal as it was found to be larger in amplitude allowing for easier recognition of peaks representative of the cardiac cycle.

The peak detection algorithm chosen to recognize these peaks was simple. A buffer containing the last 50 or so samples was continuously refreshed with new incoming sample points. Among these points, the trend of a sample point being higher in value than the value of another point a few samples ago and a few samples into the future was indicative of a peak. The width of window of time was chosen based on the analysis of the sampling frequency, as choosing a window too small would result in recognition of arbitrary peaks due to noise as heart beats. Once a heart beat was recognised, the index of the sample at which it occurred was noted. Upon recognition of another heart beat, the difference in the indices of these two beats was calculated, and knowing the sampling frequency, the time period between these two beats was deduced. This gave rise to the frequency of heart beats, which was easily converted into the units of beats per minute.

#### ***4.13 Blood Oxygen Saturation Calculation***

Acquisition and processing of data required for the calculation of blood oxygen saturation is slightly different in this project than what is suggested by research. As described all through §3.2, the idea still revolves around comparing the light absorption characteristics of oxygenated and deoxygenated haemoglobin under Red and Infrared wavelengths. However, the research that was found to do this calculation mainly described the methodology for a transmission based measurement device. It was assumed that the light intensity would be at its lowest point when the blood volume in the arteries was at its peak, and highest when the blood volume had reached its minimum. However, this

relationship is exactly the opposite in a reflectance based measurement device like the one constructed in this project, as the amount of light reflected back is the highest when there arterial blood volume is at its peak. Therefore the calculation of the ratio R, which is based on the comparison of reflected light intensities of Red and Infrared PPG signals, needed to be rethought. Since the concept of reflectance was essentially the opposite of the absorbance, it was deemed that the calculation of relationships of the various parameters in R would be inverted as follows:

$$R = \frac{\frac{DC_{\text{Infrared}}}{AC_{\text{Infrared}}}}{\frac{DC_{\text{Red}}}{AC_{\text{Red}}}} = \frac{\frac{\min(\text{PPG})_{\text{Infrared}}}{\max(\text{PPG})_{\text{Infrared}}}}{\frac{\min(\text{PPG})_{\text{Red}}}{\max(\text{PPG})_{\text{Red}}}}$$

Furthermore, the theory described in the cited research articles suggested that the DC component of the signal was needed in the computation of ratio R, as it would be used to assess the relative ratio of Red and Infrared PPG pulse heights. For this cause, the suggestion was to use two more low-pass filters with a pass band range of 0-0.5 Hz, so that the DC component of the signal could be captured separately.

However, it seemed impractical to implement these low-pass filters as it was realized that much of the motion artifact of the signal was within this range, contributing to a lot of fluctuations. If such a motion susceptible parameter were to become part of the final calculation of blood oxygen saturation, the variance of the results would be very high, resulting in a very inaccurate estimate. Since the purpose that the DC component serves in the calculation of ratio R is the comparison of relative pulse heights, it can be said that if the gains of the two signals could be adjusted to be the same, the DC component would not be needed anymore. Thus, the modified calculation of R was based on the DC offset added by the summing amplifier, which was the same for both Red and Infrared PPG signals, instead of the DC component that was inherent to the PPGs signals before being filtered.

This dependence of pulse height instead of a parallel DC component signal for the calculation of blood oxygen saturation meant that the calculation would have to be done from one heart beat to another instead of a continuous measurement. The proposition was therefore to run the IR and Red PPG signals through a peak detection algorithm as they were being acquired, so that the peaks of the heart beats could be recorded. However, it would not be efficient to run the peak detection algorithm on both the signals, especially knowing that the two PPG waveforms were temporally coincidental. Owing to the fact that they were acquired from roughly the same spatial location, and simultaneously in time, the peaks in both the PPG waves occur at exactly the same instance of time. Thus, a peak was detected in only one of the PPGs, as it could be said with high certainty that there would be a peak in the other PPG at exactly the same instance of time.

As the data processing algorithm for heart rate measurement was already running the peak detection algorithm on the Red PPG signal, the same processing results were used in this calculation too. Once two consecutive peaks were found in the Red PPG, the value of Red and IR PPGs at these two peaks were recorded. The minimum point of the signal between these two points represented the foot of the PPG wave, and this too was recorded for both Red and Infrared PPG signals. Thus, the pulse height of IR and Red PPG signals could be established and employing the formula previously discussed in this sub-section, ratio R could be calculated. Subsequently, this ratio yielded the blood oxygen saturation of the subject as a beat-to-beat impulse signal.



## **5 RESULTS AND DISCUSSION**

### ***5.1 Testing Procedures***

This project was based on test-driven design procedures. Though the methodology of the solution was conceptually designed, the practical implementation involved testing and improving each of the stages as part of its progress. Various testing procedures were part of the project even from the first phase, such as when the photodiode was tested for its sensitivity and slew rate by directing square pulses of Red and Infrared light towards it.

Luminosity of the LED lights to be used was also a concern for the success of the project as too much scatter or too little light being reflected back from the tissue meant a significantly reduced signal-to-noise ratio. Therefore, as an extension of the test of the photodiode, square pulses with various levels of DC offset were sent through the tissue to be detected by the photodiode. This not only provided an estimation of the minimum voltages required by the LEDs to be bright enough for transmittance through the tissue, but also uncovered the possibility of saturating the photodiode with too much light. It was found that the Infrared LED was too bright for the same amount of voltage as applied to the Red LED, so much so that it saturated the photodiode. The photodiode became unresponsive to changes in light intensity caused by the square pulses and produced a constant voltage signal.

Other testing procedures included comparison of active and passive band pass filters. Though active band pass filters seem to be clearly superior, passive band pass filters were found to be much easier to implement and acted as an accessory to verify the presence of the PPG waveform in the signal. Even during the implementation of the active filters as a practical addition to the circuitry, cut-off frequencies and gains were experimented with to extract an optimal PPG signal with a good signal-to-noise ratio. The constraint on this was the array of capacitors and resistors available for design, and therefore the filter constructed was optimal within the choices available.

Time multiplexing, being a significant part of the project, required the most amount of testing in order to ensure that the signals being recorded were in fact what they were supposed to be. It could very well have been possible due to improper sampling that the samples from IR and Red PPG signals were being cross-contaminated and therefore, testing procedures were devised to verify the accuracy of the sampling. Two phase testing was done to verify the functionality of time multiplexing: before and after the deconvolution of the time multiplexed signal. In the first phase, the photodiode was tested for its responsiveness with both the LEDs off. The Red LED was then connected to its time-multiplexing control signal to confirm the appearance of a “layer” of signal over the base photodiode signal. Once this layer was visible, the Red LED was disconnected and the Infrared LED was connected to its control signal. Again, the appearance of another layer of signal over the base photodiode signal was confirmed. After this, both the Red and Infrared LEDs were connected to their control signals, with the expectation of the appearance of two separate layers of signals on the base photodiode signal.

Once, this testing procedure was completed, the second phase of the testing was done after the deconvolution of the two signals through sample and hold blocks. By setting the luminosity of the Red LED to be different from that of the Infrared LED, it was confirmed that the deconvolution resulted in two distinct LED signals that were the sampled versions of the original signals. The deconvolution procedure was also tested for leakages between time slices by turning off one of the LEDs completely. The expectation of the corresponding deconvoluted signal dropping to zero was verified in order to confirm that there was no leakage from the signal of the LED that was on.

Other procedures such as longevity and stress tests were also executed on the final completed circuit in order to ensure its safety and reliability. This included leaving the circuit running for a long time as a test for possible excessive heating, and varying the supply voltage ranges from the normal range of -4.5 to 4.5V to -9 to 9 volts as test for operability under different voltage conditions (the voltage supply for the LEDs was kept constant as no infrastructure existed to automatically control their luminosity). Effects of motion were also tested on the circuitry in order to assess how long it would take the

circuit to fall back to steady state after a disturbance. Although it is expected that a better transducer design than three LEDs that were taped together (Figure 34) would greatly reduce motion artifact by clipping onto the place of measurement firmly, the transducer was shaken vigorously during signal acquisition to test for motion artifact.

Testing for the reliability of the measurements made by the device is of a completely different genre compared to those that were described thus far. To establish the accuracy of these measurements, a commercial pulse oximeter was obtained so that there may be a corroborating source of data. Once this was integrated into the testing infrastructure such that its results would be recorded in parallel with the signals produced by the circuitry of this project, various tasks were assigned to the subject to exercise these two devices. These included quick hopping in an attempt to increase the heart rate and deep, slow breaths in attempt to subsequently decrease it, push ups to decrease the oxygen saturation at the fingers (as much of oxygen would be taken up by the biceps), and hyperventilating to increase it subsequently. Although it was difficult to assess the true affects of the latter two tests on oxygen saturation, the aim was to create fluctuations in the oxygen saturation recorded by commercial pulse oximeter. The data collected was subsequently processed by the software component of this project and the results were compared with those of the commercial pulse oximeter.

## ***5.2 Circuitry Testing Results***

The results of the various test procedures executed aided in the progress and improvement of the project through out its various phases. Early implementations of the passive filters were found to produce PPG signals that were comparable to those found in the cited research. This can be seen in the picture below, which is a capture of the oscilloscope display showing the PPG signal that was acquired. The dicrotic notch of the PPG wave is clearly visible, in addition to other details such as the sharply rising systolic peak and slowly settling diastolic foot. In addition to this clarity, it should be noted that this signal, being in the range of 5V, exhibits very little noise contamination, indicating very good signal-to-noise ratio.



**Figure 25: PPG signal acquired from passive filtering**

However, the signal acquired from passive filtering was not without drawbacks. The response of the filter was very slow and it required the subject to wait approximately 5 seconds after placing the finger on the transducer for the PPG wave to appear. The signal would be saturated to  $V_{cc}$  during this initial period, and the appearance of the PPG would be marked by signal descending from  $V_{cc}$  along with the foot of the PPG. It took at least another 5 seconds for the signal to settle to baseline voltage. Furthermore, this delicate balance would once again take a long time to re-establish should the signal be disturbed by motion artifact. This extent of slowness in the system response made passive filtering very unappealing despite the quality of the signal it produced. However, it did accomplish its intended purpose of confirming the presence of a PPG signal embedded in the voltage signal received from the photodiode.

Active filter built subsequently resulted in PPG signal that was not as detailed as those produced by the passive filters. However, the response of the filter was very quick and was much less susceptible to motion artifact. This can be clearly seen in the following figure, where the recorded signal shows a motion artifact and the response of the filter in quickly adapting to it. It can be seen that the signal momentarily saturates the signal to  $V_{cc}$ , but quickly returns to show the PPG waveform. It was found that even the saturating

response to the motion artifact would disappear to a good measure if the motion was fast and prolonged.

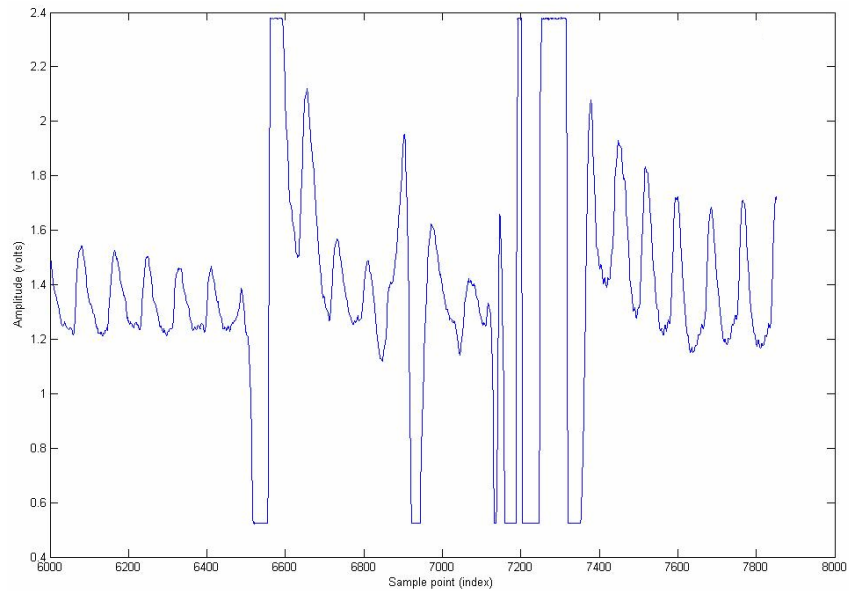


**Figure 26: Filter response to motion artifact in PPG signal**

Testing and experimenting with the timing circuits (§4.9) was especially interesting as it brought about the fundamental concepts of modulation and sampling to the surface. As described in the previous section, the outlined testing procedures had an expectation of seeing layered signals from the photodiode channel in response to time multiplexing. This can be clearly seen in the results obtained from the test, which are shown as a capture of the oscilloscope display in the following figure.

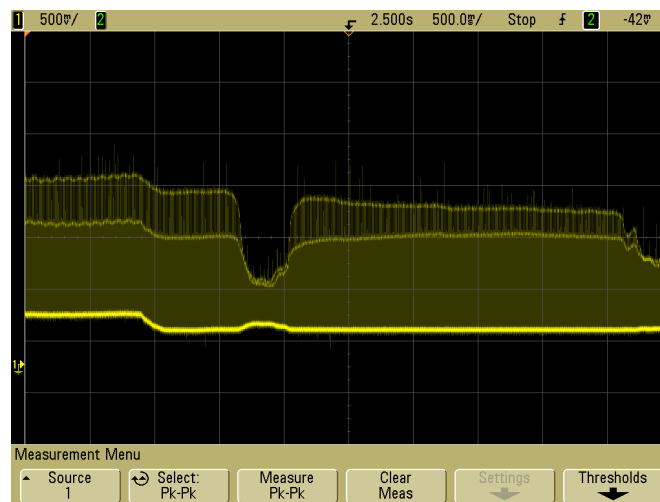


**Figure 27: Multilayered time-multiplexed signal**

The time-multiplexed signal that is shown in the above figure is exhibiting three layers that are occurring seemingly simultaneously. The bright bottom baseline signal is representative of the response of photodiode to the ambient light. The lighter layer superimposed on top of this is the response of photodiode to impulses of Red light. The even light layer which is at the top of these two is the response due to impulses of Infrared light. The changing intensity of layers suggested that even though these layers appear simultaneous, they are not so in reality and the intensity is proportional to the density of the impulses. This was easily confirmed by spreading out the time axis to produce the following output from the oscilloscope.

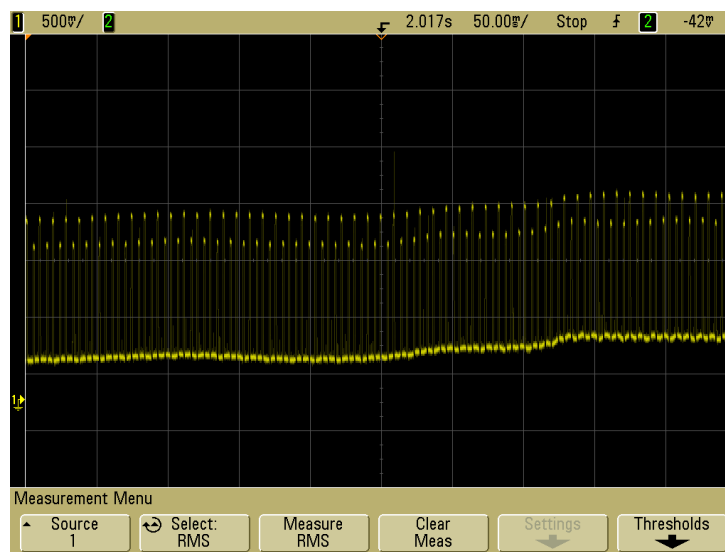


**Figure 28: Time slicing in multiplexed signal**

The impulses of Red and Infrared light are clearly separated in time and are modulated in their amplitude by the environment they are passing through. This not only confirmed the successful functioning of time multiplexing, but also allowed a comparison of amplitudes of Infrared and Red signals. It can be seen in Figure 27 that the two layers dip down to become coincidental for a brief period of time. This was part of the testing procedure to see the response of photodiode when the light was passing through the tissue to it. By becoming coincidental, the layers confirmed that the luminosity of Red and Infrared lights were approximately the same while passing through the finger.

### 5.3 Heart Rate Data Processing Results

As discussed in §4.11, due to lack of sufficient throughput in the TCP/IP server distributing the data acquired via Bluetooth, the signals received by the TCP/IP clients were under-sampled. It was deemed best to pipeline the data acquired from the serial port to files for post processing. However, since the algorithms designed were based on the assumption of real-time data acquisition, the data processing can still be considered real-time.

Peak detection algorithm that was implemented was capable of identifying peaks very well, even under testing conditions simulating faster heart beats. In addition to this, false detection of dicrotic notch as a peak was a concern that needed to be verified. The algorithm succeeded in detecting only the true heart beat peak most of the time, thus proving that the implementation was a reliable way to calculate heart rate. The results of the algorithm when executed on a sample of data are shown in the following figure.

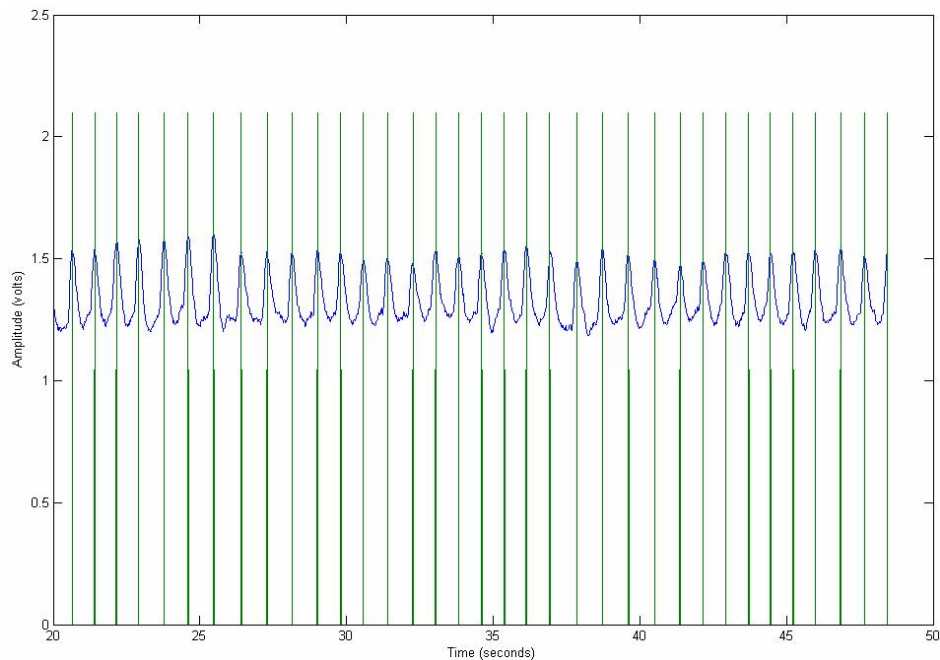


**Figure 29: Impulses embedded in PPG showing detected peaks**

Since the sampling frequency of data acquisition was found to be about 1 KHz, the heart rate was calculated first as frequency and then converted to beats per minute. In regards to the experiment did by the subject to exercise the commercial and project measurement devices, the following results of the calculation of heart rate compare the two devices.

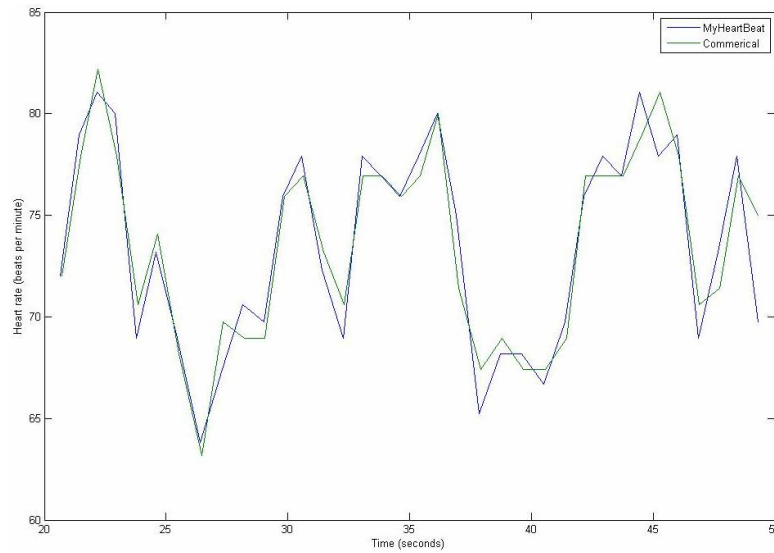


**Figure 30: Beat-to-beat heart rate calculations of commercial and project devices**

It can be seen in the above figure that the calculation of heart rate based on the data from the project matches well with that of the calculations based on the commercial pulse oximeter's data. In order to assess the performance of the algorithm at faster heart rates, the subject was asked to exercise and increase their heart rate. The results for this test are shown in the following figure.

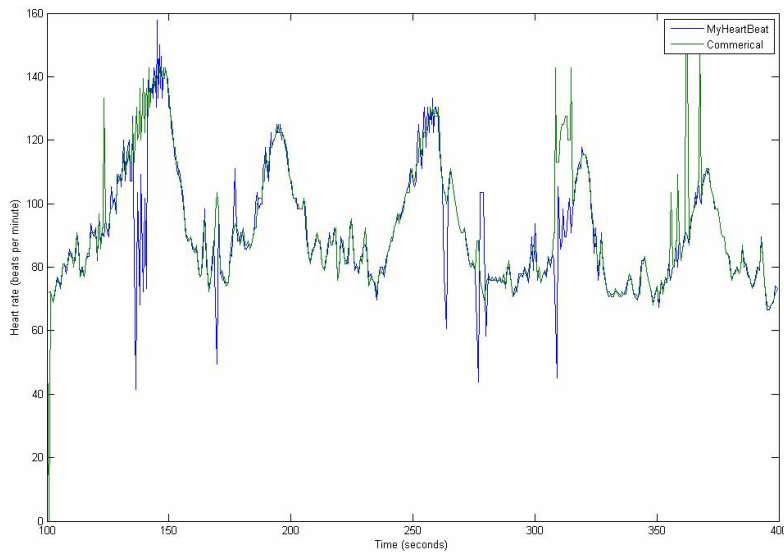


**Figure 31: Heart rate during exercise cycles**

The five cycles of heart rate that are shown in the above figure represent the affect of exercise of the subject on the heart rate. Heart rate starts from a moderate value of about 75bpm and rises to 140bpm in about 100 seconds as a result of the subject hopping quickly. Subsequent deep and slow breaths bring the heart rate down to a value of about 80bpm. This cycle was repeated 5 times over the course of 5 minutes, and this



representation can be clearly seen in the figure. The sudden sharp peaks in the recording are attributed to the motion artifact of hopping quickly. However, the data is still much less contaminated by motion artifact considering that the subject was exercising vigorously.

#### 5.4 Blood Oxygen Saturation Data Processing Results

Processing of data for blood oxygen saturation was done by collecting the Red and IR PPG data in conjunction with the output of the commercial pulse oximeter. The pulse oximeter produced a voltage signal between 0 and 1 volt as a representation of blood oxygen saturation (0-100%). Therefore, the output value of the project was also decided to be between 0 and 1, so that the two values could be compared without modification to the output signal of the pulse oximeter. The following figure shows the results of processing of a sample of data that was received from the two devices.

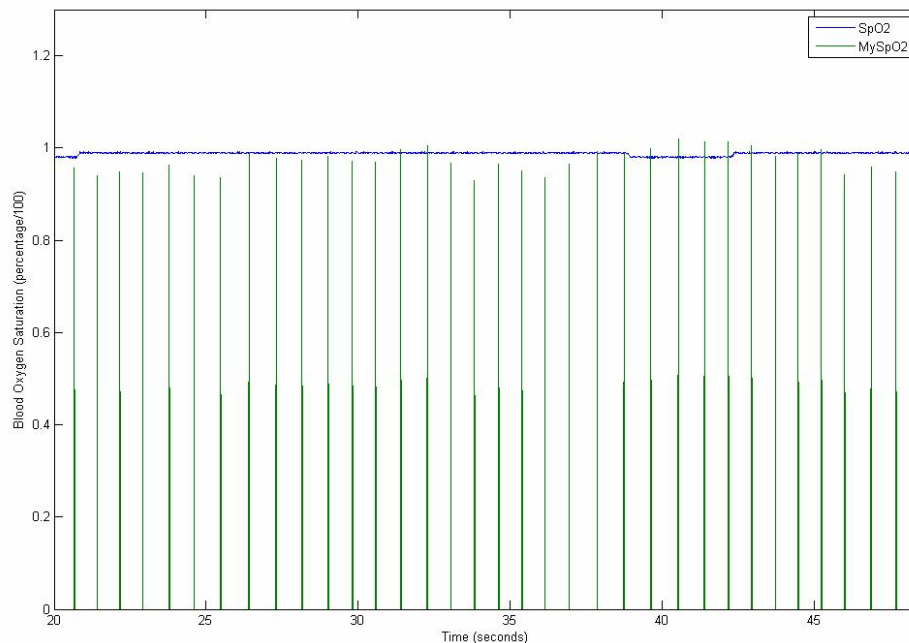


**Figure 32: Blood Oxygen Saturation calculation results**

One of the first things noticeable from the above graph is that the blood oxygen saturation that was obtained from the commercial pulse oximeter is a continuous signal where as the one computed in the project is an impulse train. As discussed previously (§4.13), this is because the algorithm calculates blood oxygen saturation on a beat-to-beat basis. Furthermore, the signal from the commercial pulse oximeter is a windowed average of the real-time oxygen saturation, unlike the results of this project. However, it

can be seen in the above graph that the results are still comparable to those of the commercial pulse oximeter. When the subject was asked to perform tasks such as exercising and hyperventilating, the blood oxygen saturation readings from the two devices changed and this can be seen in the following figure.

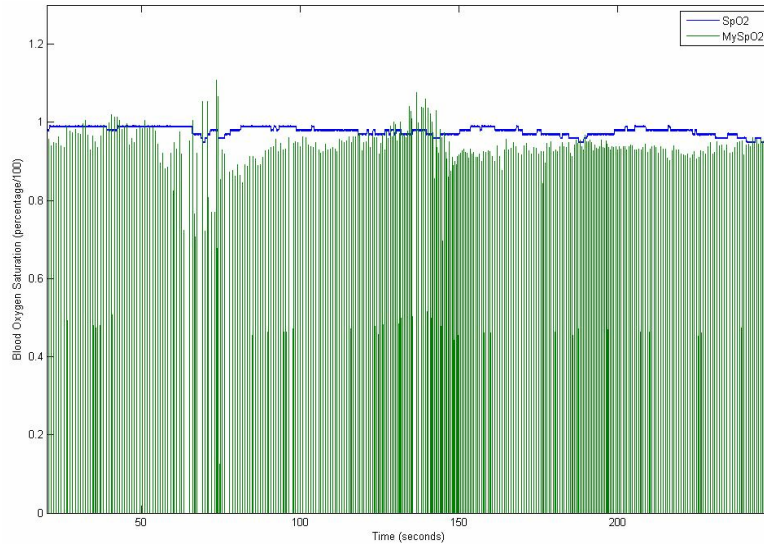


**Figure 33: Blood oxygen saturation during exercise cycles**

It can be seen in the figure above that the oxygen saturation fluctuates slightly. However, the oxygen saturation does not dip down to extreme values during the exercise and is around 96% most of the time, perhaps because the subject was healthy. Although the general trend of decreasing oxygen saturation can be seen in both project and commercial oximeter data (results of first 50 seconds compared to results after 150 seconds), the agreement of results could have been better between the two. This difference in results could be attributed to various factors such as the more robustly designed and tested processing algorithm of the commercial pulse oximeter, the decision to not include the DC component in the calculation of ratio  $R$  in this project, and the use of different spatial locations for PPG signals of the project's circuit and the commercial device. Commercial pulse oximeters base their outputs on lookup tables for ratio  $R$  which are built from several clinical trials and are therefore, not equivalent to theoretical results. The lack of such infrastructure in execution of this project can be a reason why there is discrepancy between the two results, albeit a minor one. Additionally, it can also be said that the decision to not include the DC component of the PPG waves in the calculation of  $R$  as

suggested by theory contributed to the inaccuracy in the results. However, inclusion of the DC component could have resulted in even less accurate results due to its increased susceptibility to motion artifact. Also, the fact that the blood oxygen saturation readings of the two devices were obtained from two different fingers (due to space constraints) may be a minor factor that added to the disagreement between the two.

## 6 CONCLUSIONS AND RECOMMENDATIONS

Availability of a year's time to plan, design and build this project from scratch was a definite contributor to its success, if it can be seen as so. The numerous challenges encountered during this time only improved the design procedures and can be seen as necessary catalysts.

The biometrics of heart rate and blood oxygen saturation produced by this device are important additions to NIHMS and serve as significant indicators of the health of the individual. The availability of real-time data such as these to an average user can impact their perspective of their health status, allowing them to detect deteriorating conditions earlier on and take necessary precautions. Although the accuracy of the measurements such as the blood oxygen saturation may not be clinically acceptable, they are still very close to the actual results and can be used in trend analysis if not in clinical diagnosis. The possibility of extracting a rich trend from the data samples acquired over a long time outweighs the minor inaccuracies in the data collected. The strength of this project lies in the portability and remoteness of the acquisition of these biometrics.

If given more time to work on this project, the project could be further improved in various ways. The implementation of the data reception system on the processing centre would be written in a more powerful and fast language such as C. The throughput of the TCP/IP server would be significantly increased thus, to allow for richer parallel data acquisition by remote clients. This would make the data processing truly real-time. In regards to improving the accuracy of the results, the software would be modified to detect and handle common artefacts. For example, uncommon and transient extreme heart rates can be regarded as motion artifact and be filtered out. A windowed average could smoothen the fluctuations in the beat-to-beat heart rate measurement, producing a stable output to the user. Implementation of DC component filters in hardware could be explored in an attempt to improve the accuracy of blood oxygen saturation. This biometric would be also subject to a windowed average to smoothen out its fluctuations and produce a continuous signal rather than an impulse train. Logistical improvements

such as building a better and more stable transducer can significantly filter out motion artifact and improve accuracy of the measurements.

In terms of making the device more portable, the device would be miniaturized onto a printed circuit board making it light weight and more stable. Additionally, a regulated power source based on AA or 9V batteries would be built to allow for mobility. As other transducers of NIHMS could be attached to the subject in any location, the data acquisition system is expected to become decentralized. In such a scenario, it would be impractical to input the collected signals through wires to the data acquisition system. Therefore, localised data acquisition systems that are part of the PCB of this device could be built that wirelessly transmit the signals collected to the decentralized data acquisition system or directly to the processing centre.

Furthermore, the decision to use a reflectance based transducer for data collection allows this project to be used on any area of the body where the vasculature is close to the skin surface. During the course of this project, acquisition of PPG signals from the wrist was attempted and was successful, although with increased susceptibility to motion artifact. Therefore, a compact device of the size of a watch is envisioned, one that does not need to get its signal from the fingers, thus freeing them up to their normal use.

In conclusion, the project can be further improved in various ways that can make it more portable, user-friendly and accurate. It can become a good accessory to the user in tracking their health and the health of the ones they are concerned about. It can also become a good addition to the automated infrastructures already in place in hospitals that provide real-time data remotely to the doctors.

## 7 APPENDIX A: HARDWARE COST AND PROTOTYPE

Parts that were used in the prototyping the project are listed below. Though the cost of building this prototype is calculated to be \$34.51, additional quantity of these and other types of parts were purchased as part of the development phase. Therefore, the total budget of the project can be estimated to be around \$50.

<b>Part Name</b>	<b>Qty</b>	<b>Total Part Price (CAD \$)</b>
555/556 Timer – NE556N	1	0.65
Decade Counter – HCF4017BE	1	1.04
Sample Hold – LF398N	2	4.70
Quad Op-amps – LM324N	2	1.06
Quad Bilateral Switch – CD4066BE	1	0.74
Photodiode – PNZ334	1	1.97
Red LED – SSL-X5093SRC/DV	1	0.38
Infrared LED – LTE-5208A	1	0.32
Breadboards – TW-E40-1020	2	24.10
<b>Total Price</b>		<b>34.51</b>

**Table 2: Bill of Materials**

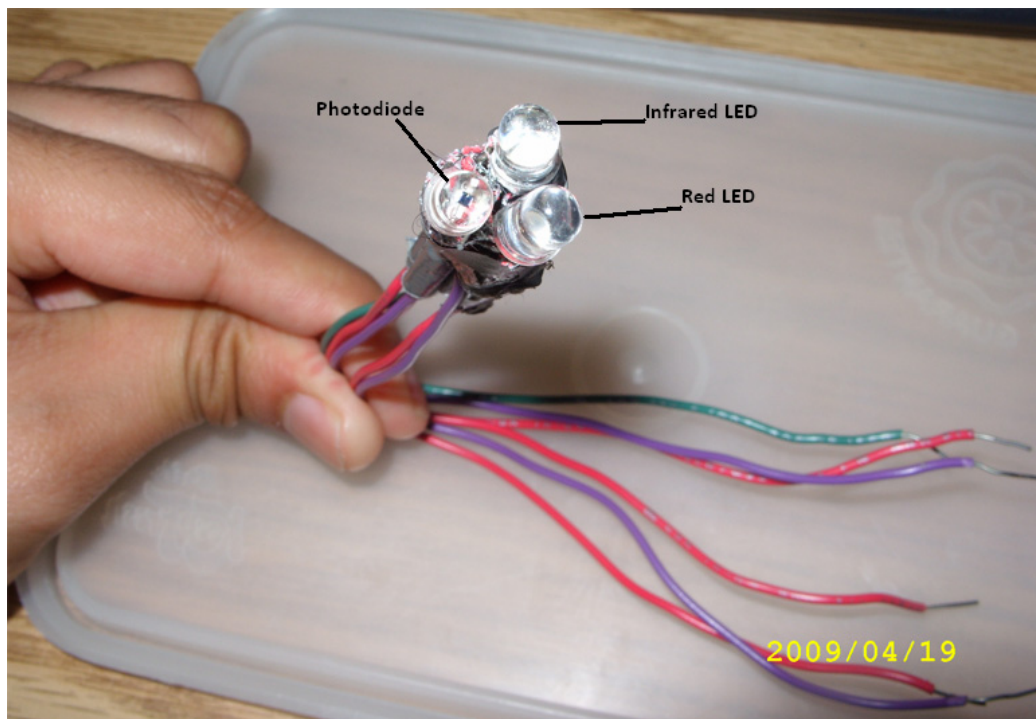


Figure 34: PPG signal transducer

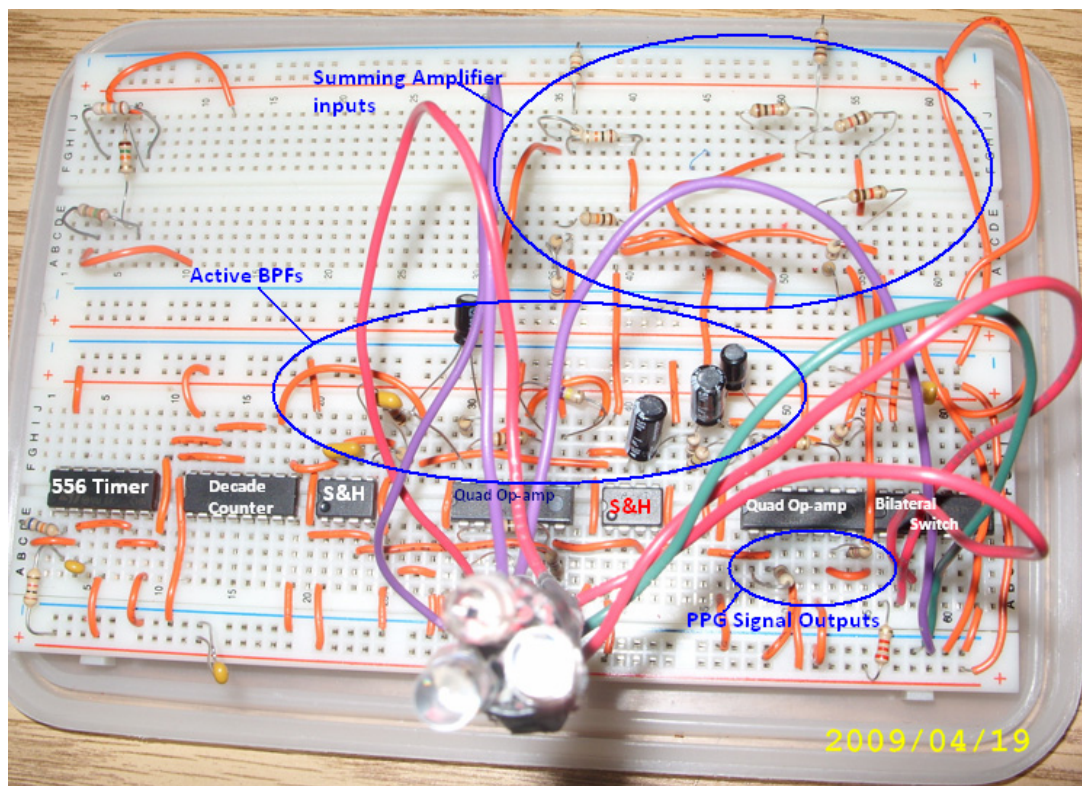


Figure 35: Prototype Circuit Board

## 8 APPENDIX B: DATA PROCESSING SOFTWARE

### 8.1 MATLAB Processing Code

Signals were processed in MATLAB R2007b that was available as part of lab resources in the course. The following is the code that was written to produce the biometrics of heart rate and blood oxygen saturation.

```
clear all;
close all;
clc;
%Load data collected
load finaldata.txt
Red=finaldata(:,1); %Extract out each of the signals
IR=finaldata(:,2);
Ext=finaldata(:,3); %Commercial Oximeter PPG wave ("External" PPG)
spo=finaldata(:,4); %Commercial Oximeter SpO2
clear finaldata;

%Define Extinction Coefficients
eHbORed=0.08;
eHbRed=0.81;
eHbIR=0.18;
eHbOIR=0.29;

%Initialize Peak Detection Variables
peaks(1)=0; %This is where the impulses will be placed in response to detected
heart beat
peaks(2)=0;
peaksext(1)=0; %Same kind of array for external PPG
peaksext(2)=0;
peakcount=0; %Count of peaks detected
peakcountext=0; %Count of peaks detected in external PPG
previousk=1;
previouskext=1

from=2000; %Option of choosing the range of data samples to process
heartbeat(1)=72; %Initialize first sample of heart rate (because we don't have
a previous peak to calculate this from).
heartbeaext(1)=72;
sample=10e-3;

for k=from:25000
    if (Red(k)>1.4) %If Red PPG is greater than a threshold...
        %...and demonstrates an inflection point ...
        if (Red(k)>Red(k-5) && Red(k-5)>Red(k+5) && k>(previousk+10))
            peakcount=peakcount+1; %...then we have a peak
            peaks(k)=2.1; %Put an impulse there (just for visual purposes)
            peaksat(peakcount)=k; % Note down its index
            if (peakcount>=2) %If we have more than 1 peak
                pulselow(peakcount-1,1)=min(Red(peaksat(peakcount-
1):peaksat(peakcount))); %calculate the low point between two peaks
                pulselow(peakcount-1,2)=min(IR(peaksat(peakcount-
1):peaksat(peakcount)));
                %Calculate ratio R
                R=log(pulselow(peakcount-1,2)/IR(peaksat(peakcount-
1)))/log(pulselow(peakcount-1,1)/Red(peaksat(peakcount-1)));
                %calculate SpO2
```



```

        myspo(peakcount-1) = ((eHbRed-eHbIR*R) / ((eHbRed-
eHbORed) + ((eHbOIR-eHbIR)*R)));
        %caculate heart rate
        heartbeat(peakcount)=60/((k-previousk)*sample);
        %Crude filtering of motion artifact: ignore all heart rates
        % > 160
        if heartbeat(peakcount)>160
            heartbeat(peakcount)=heartbeat(peakcount-1);
        end
    end
    previousk=k;
end
else
    peaks(k)=0;
end
%Run heart rate calculation on external PPG too, for comparison
if (Ext(k)>0.5)
    if (Ext(k)>Ext(k-5) && Ext(k-5)>Ext(k+5) && k>(previouskext+10))
        peakcountext=peakcountext+1;
        peaksext(k)=2.1;
        peaksatext(peakcountext)=k;
        if (peakcountext>=2)
            heartbeatext(peakcountext)=60/((k-previouskext)*sample);
            if heartbeatext(peakcountext)>160
                heartbeatext(peakcountext)=heartbeatext(peakcountext-1);
            end
        end
    end
    previouskext=k;
end
else
    peaksext(k)=0;
end
end

%Plot the data
to=peaksat(peakcount-1);
figure
plot(from:to,Red(from:to)+1,from:to,IR(from:to),from:to,Ext(from:to));
xlabel('Time (seconds)');
ylabel('Amplitude (volts)');
h = legend('Red','IR','Ext',1);
figure
plot((from:to)*sample,spo(from:to),(from:to)*sample,myspo(from:to));
h = legend('SpO2','MySpO2',1);
axis([from*sample to*sample 0 1.3]);
xlabel('Time (seconds)');
ylabel('Blood Oxygen Saturation (percentage/100)');
figure
plot(peaksat*sample,heartbeat,peaksatext*sample,heartbeatext);
h = legend('MyHeartBeat','Commercial',1);
xlabel('Time (seconds)');
ylabel('Heart rate (beats per minute)');

```

## 8.2 Ruby TCP/IP Server code

### Serial.rb

```

require 'Win32Serial'
port = Win32Serial.new
port.open("COM4")
file1=File.new("datafile1.txt", "w+")
file2=File.new("datafile2.txt", "w+")

```

```

file3=File.new("datafile3.txt", "w+")
file4=File.new("datafile4.txt", "w+")
# 9600 baud / 8 bytesize / no parity / 1 stopbit
port.config(9600, 8, Win32Serial::NOPARITY, Win32Serial::ONESTOPBIT)
# optionally configure timeouts
port.timeouts(0, 200, 0, 0, 0)
char="C"
puts "Reading"
streamSock = TCPSocket.new( "127.0.0.1", 21000 )
while true do
  while (char != "B") do
    char=port.read(1)
  end
  char="C"
  line=port.read(20);
  streamSock.puts(line);
  data=line.split(/;/);
  file1.puts data[0]
  file2.puts data[1]
  file3.puts data[2]
  file4.puts data[3]
end
port.close
streamSock.close;
file1.close
file2.close
file3.close
file4.close

```

### **Server.rb**

```

require "socket"
require 'Win32Serial'
require 'thread'
dts = TCPServer.new('localhost', 20000)
serialS= TCPServer.new('localhost', 21000)
mutex=Mutex.new
Thread.start(serialS.accept) do |s|
  puts "Serial Reader Connected!"
  loop do
    begin
      mutex.synchronize{
        $str=s.gets;
      }
    rescue StandardError
      puts "Socket error. Serial Reader may have terminated the connection."
      serialS.close
      dts.close
      break;
    end
  end
end

loop do
  Thread.start(dts.accept) do |s|
    #prevcount=-1;
    print(s, " is accepted\n")
    loop do
      begin
        resp=s.recv(1);
        mutex.synchronize{
          data=$str.split(/;/);

```

```
    if (resp=="A")
      value=[data[0].to_i].pack("N");
    elsif (resp=="B")
      value=[data[1].to_i].pack("N");
    elsif (resp=="C")
      value=[data[2].to_i].pack("N");
    elsif (resp=="D")
      value=[data[3].to_i].pack("N");
    else
      value=[data[0].to_i].pack("N");
    end
    s.write(value)
  }
rescue StandardError
  puts "Socket error. Client may have terminated the connection."
  break
end
end
print(s, " is gone\n")
s.close
end
end
```

## 9 REFERENCES

- [1] G. M. Azmal, A. Al-Jumaily and M. Al-Jaafreh, "Continuous Measurement of Oxygen Saturation Level using Photoplethysmography Signal," *Biomedical and Pharmaceutical Engineering, 2006. ICBPE 2006. International Conference on*, pp. 504-507, 2006.
- [2] Guowei Di, Xiaoying Tang and Weifeng Liu, "A Reflectance Pulse Oximeter Design Using the MSP430F149," *Complex Medical Engineering, 2007. CME 2007. IEEE/ICME International Conference on*, pp. 1081-1084, 2007.
- [3] R. C. Gupta, S. S. Ahluwalia and S. S. Randhawa, "Design and development of pulse oximeter," *Engineering in Medicine and Biology Society, 1995 and 14th Conference of the Biomedical Engineering Society of India. an International Meeting, Proceedings of the First Regional Conference. , IEEE*, pp. 1/13-1/16, 1995.
- [4] J. Lee, W. Jung, I. Kang, Y. Kim and G. Lee, "Design of filter to reject motion artifact of pulse oximetry," *Computer Standards & Interfaces*, vol. 26, pp. 241-249, 5. 2004.
- [5] Y. Sterlin, "Specific problems in the development of pulse oximeters," *Biomed. Eng.*, vol. 27, pp. 336-341, 11/01. 1993.
- [6] R. Stojanovic and D. Karadagic, "A LED-LED-based photoplethysmography sensor," *Physiol. Meas.*, vol. 28, pp. N19-N27, 2007.
- [7] D. Traviglia and Y. Mendelson, "A portable setup for comparing transmittance and reflectance pulse oximeters for field testing applications," *Bioengineering Conference, 2004. Proceedings of the IEEE 30th Annual Northeast*, pp. 212-213, 2004.
- [8] G. Uretzky and Y. Palti, "A method for comparing transmitted and reflected light photoelectric plethysmography," *J. Appl. Physiol.*, vol. 31, pp. 132-135, /7/1. 1971.
- [9] G. A. Zaleskaya and E. G. Sambor, "Interaction of Low-Intensity Laser Radiation with Blood and Its Components," *Journal of Applied Spectroscopy*, vol. 72, pp. 242-248, 03/01. 2005.
- [10] S. A. A. P. Hoeksel, J. R. C. Jansen, J. A. Blom and J. J. Schreuder, "Detection of Dicrotic Notch in Arterial Pressure Signals," *J. Clin. Monit. Comput.*, vol. 13, pp. 309-316, 09/01. 1997.

## 10 VITAE

NAME: Yousuf Jawahar

PLACE OF BIRTH: Hyderabad, India

YEAR OF BIRTH: 1987

SECONDARY EDUCATION: Lincoln M. Alexander Secondary School  
(2001-2004)

UNDERGRADUATE EDUCATION: Electrical and Biomedical Engineering  
(2004-2009)

WORK EXPERIENCE: Software Developer – Certicom Corp  
(2007-2009)

HONOURS AND AWARDS: Queen Elizabeth Aiming for the Top  
Scholarship (2004-2009),  
Apotex Scholarship (2004-2009),  
University Senate Scholarship (2006),  
H.L. Hooker Scholarship (2008),  
Dean's Honour List (2004-2009)